

KATHOLIEKE
UNIVERSITEIT
LEUVEN

NECESSITY FROM CHANCE: SELF-ORGANIZED REPLICATION OF SYMMETRIC PATTERNS THROUGH SYMMETRIC RANDOM INTERACTIONS

André Barbé

SCD/SISTA report nr. 08-53
April 2008

INGENIEURSWETENSCHAPPEN
Departement Elektrotechniek (ESAT-SCD)
Kasteelpark Arenberg, 10
B3001 Leuven /Heverlee - Belgium

Necessity from Chance: Self-Organized Replication of Symmetric Patterns through Symmetric Random Interactions

A. Barbé

Department of Electrical Engineering, Katholieke Universiteit Leuven
Kasteelpark Arenberg 10, B3001 Leuven, Belgium

Abstract

We present an algorithm, completely random in nature, that, without invoking a fitness function or purposeful design, produces symmetric replicas in a population of so-called cellicules. Cellicules consist of "cells" arranged in a structure with geometric symmetry S. Each cell has one of two possible states, thus defining a state-configuration pattern on a cellicule. The algorithm acts recurrently on a population of cellicules, possibly randomly initialized, through a random "copying interaction" between two randomly selected cellicules that first undergo a random reorientation in accordance with the symmetry S. The dynamics of the algorithm is analyzed in detail for several symmetries. This shows that it is a random walk with absorbing states which correspond to a population in which all cellicules have an identical S-symmetric configuration pattern. We discuss some aspects concerning the evolution of cellicule-populations under mixing and mutation, and some variations on the basic algorithm.

Keywords: self-organization, artificial chemistry, emergent behaviour, complexity, evolution, random walk, gambler's ruin, mixing populations, sociodynamics, statistical physics, pattern formation.

1 Introduction

Since a couple of decennia, several kinds of games and algorithms have been devised that mimic life and evolution processes, and which have induced research domains known as artificial life [Langton, 1997], evolutionary computation (with a.o. genetic algorithms) [de Jong, 2006]. All of them have some flavor of reproduction, possibly under random mutation followed by subsequent selection of the offspring that is best fit. In many cases this involves an explicit fitness function, a source of much controversy in the evolution debate (cf. Dawkins' Weasel program ([Dawkins, 1986])). These algorithms are reminiscent of the neo-Darwinist view where evolution is dominated by the role of mutating and surviving ("naturally selected") genes. Some authors (see e.g.,[Kaufmann, 1993], [Stewart, 2003]) argue that self-organization should be given a role in evolution. Although still a controversial issue in natural evolution, it is not the case in the context of artificial life. It has even inspired the development of evolutionary optimization algorithms, such as "ant" and "swarm"-algorithms, which mimic the self-organization in insect colonies [Dorigo & Stutzle, 2004][Engelbrecht, 2005].

Staying in an artificial context in which one can study "what might be, in order to be able to discover what is" (quoting [Stewart, 2003]), we introduce and analyze here an experiment in which a population of initially randomly patterned objects evolves spontaneously, through random interactions between its members, towards a population where

all members show an identical symmetric pattern. And this without referring to an explicit fitness function or some purpose. Instead, it is the intrinsic symmetry of the shape of the objects, which also defines the random interactions, that forms the implicit driving force for this self-organized pattern formation (in the sense defined by [Camazine *et al.*, 2001], p.8).

Our experiment fits well in the domain of *artificial chemistry*, a subdomain of artificial life [Dittrich *et al.*, 2001]. An artificial chemistry is defined by a triple $(\mathcal{C}, \mathcal{D}, \mathcal{I})$. $\mathcal{C}$ represents a set of "molecules", i.e. objects that can interact with each other to form new objects in $\mathcal{C}$. $\mathcal{I}$ defines the possible interactions ("reactions") between elements of $\mathcal{C}$, and $\mathcal{D}$ specifies the dynamics which determines which "molecules" in a certain population (soup, reaction vessel) $\mathcal{P}$ are made to interact.

Cellicules. *"Cellicule"* is an artificially constructed word, obviously contracting "cellular" and "molecule", which is used for an agglomerate of artificial cellular objects (cells) which are arranged in a particular shape. Examples of cellicules are shown in Figure 1, where cells are represented by circles. For convenience, we only consider "planar" cellicules in our experiments and illustrations. The *size* of a cellicule refers to the number of cells it contains.

The shape of a cellicule has some symmetry S, i.e. it is invariant under the action of some symmetry group S, as illustrated in Figure 1 (this Figure also reminds of the Z_1-,Z_2-,Z_3-,D_3-,D_4- and D_6-symmetries. Note that we hereby consider an absolute orientation of the cellicules with respect to an external reference frame. E.g., triangular cellicules will generally be represented top down with respect to the page-frame, string-cellicules horizontally.

Each cell in a cellicule is attributed a state from a binary set, say $\{0, 1\}$. In that way, each cellicule has a certain *state configuration pattern* associated with it. A state configuration will also be considered in relationship to the external reference frame. The configuration itself need not be S-symmetric. This means that a cellicule with an S-symmetric shape can reorient under the action of any operation in S, which leaves the shape invariant (with respect to the reference frame), but generally results in a new configuration (with respect to the reference frame). Figure 1 shows the possible reorientations for so-called string-cellicules and triangular cellicules.

Given a fixed cellicule shape and size, the set

$$\mathcal{C} = \{c_1, c_2, \ldots, c_L\}$$

consists of all cellicules with that particular shape and size, but with distinct configurations (with respect to the reference frame). Thus it makes sense to say that under an S-induced reorientation, a cellicule in $\mathcal{C}$ generally transforms into another cellicule in $\mathcal{C}$.

A population $\mathcal{P}$ containing N cellicules is an indexed family

$$\mathcal{P} = \{C_j\}_{j=1,\ldots,N}, \quad \text{with} \quad C_j \in \mathcal{C} = \{c_1, c_2, \ldots, c_L\}. \tag{1}$$

As it may happen that $C_i = C_j$ when $i \neq j$, this corresponds to a *multiset*

$$\mathcal{P} = \{c_1(n_1), c_2(n_2), \ldots, c_L(n_L)\}, \tag{2}$$

where n_j is the multiplicity of cellicule c_j in $\mathcal{P}$. Note that $n_1 + n_2 + \ldots + n_L = N$.

The dynamics $\mathcal{D}$ and the interaction $\mathcal{I}$ are implicitly defined in the algorithm presented in the next section.

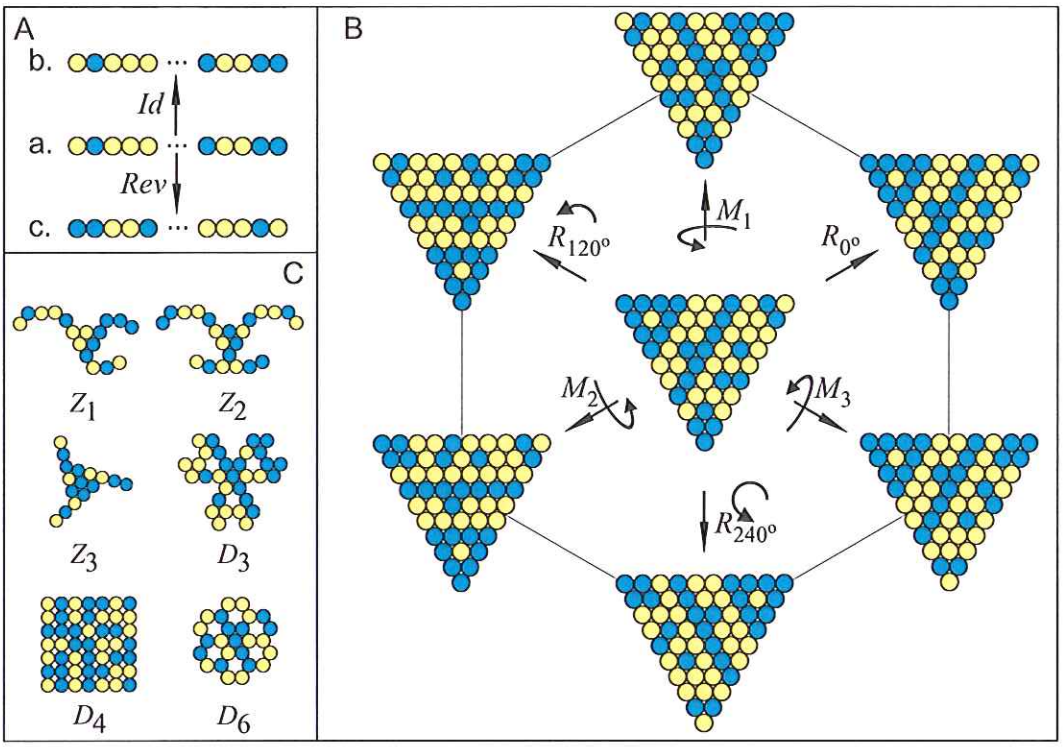


Figure 1: **(A)** String-cellicules having Z_1- and Z_2-symmetric shape. Z_1 is the symmetry group with the identity Id as single element. Z_2 is the cyclic group containing Id and Rev (reverse). A(b) and A(c) illustrate how Id and Rev operate on the cellicule in A(a): the shape remains unchanged, but a state configuration on the cellicules generally changes under the corresponding operation. **(B)** A triangular cellicule with dihedral D_3-symmetric shape: $D_3 = \{R_{0°} = Id, R_{120°}, R_{240°}, M_1, M_2, M_3\}$, where $R_{\alpha°}$ denotes a counterclockwise rotation by $\alpha°$ and M_1, M_2, M_3 denote reflections along the medians, as illustrated. Note that the cyclic group $Z_3 = \{R_{0°}, R_{120°}, R_{240°}\}$ is a subgroup of D_3, as well as $Z_1 = \{R_{0°}\}$ and $Z_2 = \{Id, M_i\}, (i = 1, 2, 3)$. **(C)** A selection of cellicules with alternative shapes having the indicated symmetries.

2 Necessity from Chance

The title of this section is of course reminiscent of J. Monod's once controversial book *Chance and Necessity* [Monod, 1972]. Here it emphasizes the fact, as will be demonstrated, that random (chance) cellicule-interactions which exploit the intrinsic shape-symmetry of the cellicules, produce inevitably (by necessity) a population of well-structured (symmetric) replicas.

2.1 Chance: the S-algorithm, implementing intrinsically symmetric random interactions

Here follows a formal description of the S-algorithm, where S refers to a symmetry (group) describing the symmetry of the cellicule's shape. One iteration of the algorithm is, by way of example, explained and illustrated in Figure 2(A) for a population of triangular cellicules and $S = D_3$. $\mathcal{C} = \{c_1, c_2, \ldots, c_L\}$ denotes the set of all cellicules of the same size and with S-symmetric shape, but with distinct configurations (w.r.t. the reference frame).

The S-algorithm

step 1 (initialization): Initialize a population $\mathcal{P}$ of N cellicules. The configuration of these cellicules may (but need not) be generated randomly.

step 2 (implementation of the dynamics $\mathcal{D}$) :

step 2.1 : select randomly and independently two *parent* cellicules from $\mathcal{P}$, say C_a and C_b (for some distinct $a, b \in \{0, ..., N\}$).

step 2.2 : select randomly and independently two operations $\delta_1, \delta_2 \in S$ (with equal probability $|S|^{-1}$), and let them act on C_a and C_b respectively, thus producing as outcome the cellicule pair

$$(\delta_1(C_a), \delta_2(C_b)) \in \mathcal{C}^2.$$

step 2.3 (alignment) Align $\delta_1(C_a)$ and $\delta_2(C_b)$, i.e. bring all cells in both cellicules in the natural 1-1 correspondence which is obtained by an exact juxtaposition of the cellicules.

step 3 (implementation of the interaction $\mathcal{I}$)

step 3.1 (interaction in the pair through bilateral random copying): This step makes $\delta_1(C_a)$ and $\delta_2(C_b)$ interact through aligned pairs of cells, and produces a pair of identical cellicules, according to the following rule:

For *each* cell in $\delta_1(C_a)$, find the corresponding aligned cell in $\delta_2(C_b)$. Then,

- if both cells are in the same state: leave them in this state
- if both cells have a different state: bring both cells into a state 0 with probability ν_0, or into state 1 with complementary probability $\nu_1 = 1 - \nu_0$.

This can be thought of as a bilateral random copying between $\delta_1(C_a)$ and $\delta_2(C_b)$, in which a cell in state 1 copies the 0 of its aligned neighbour with probability ν_0 (or equivalently: a cell in state 0 copies its neighbour's 1 with probability ν_1). "Bilateral" refers to the fact that there is no hierarchy between interacting cellicules. If aligned cells in $\delta_1(C_a)$ and $\delta_2(C_b)$ have the same state, they are already each other's copy.

Each cellicule in the identical pair thus obtained will be denoted

$$R(\delta_1(C_a), \delta_2(C_b)).$$

step 3.2 (population update)

Let $C_a = C_b = R(\delta_1(C_a), \delta_2(C_b))$, i.e. replace the parent cellicule pair (C_a, C_b) in the population by the identical twin obtained in step 3.1, thus producing a (possibly) modified population.

In the chemistry metaphor, this interaction can be symbolically represented by the reaction equation

$$C_a + C_b \rightarrow 2R(\delta_1(C_a), \delta_2(C_b)), \tag{3}$$

step 4 (closing the loop): return to step 2.

Note that the dynamics $\mathcal{D}$ implemented in step 2 mimics the behaviour of molecules in a well-stirred reactor: cellicules reorient randomly and meet randomly in pairs, after which they interact under proper alignment. This is metaphorically illustrated in Fig. 2(B).

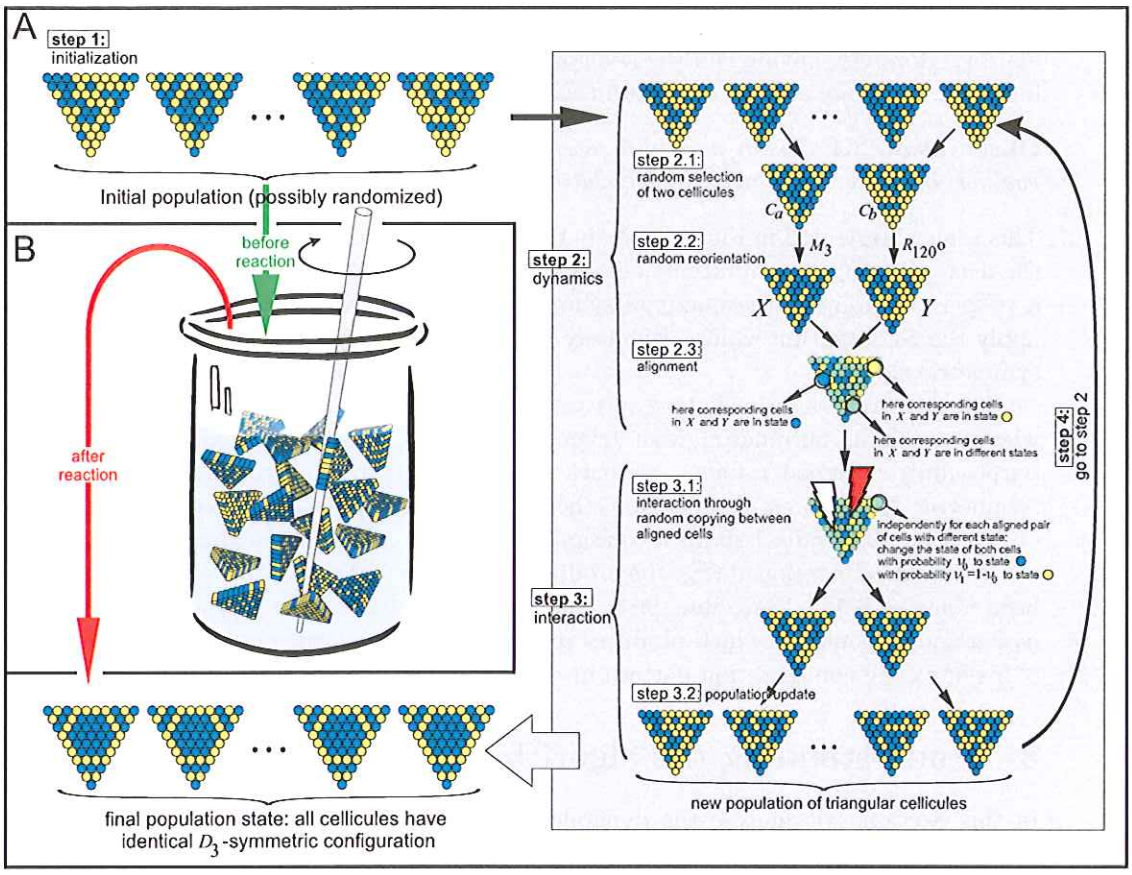


Figure 2: **(A)** The distinct steps in the S-algorithm, illustrated for $S = D_3$. Step 1 initializes the population of cellicules (possibly randomly). Step 2 implements the dynamics $\mathcal{D}$: it selects a random pair of "parent" cellicules C_a and C_b(substep 2.1), and performs an independent random reorientation on each parent, yielding the cellicules X and Y (substep 2.2). These reorientations are taken from the six elements of the symmetry group D_3, each with equal probability 1/6. After that, X and Y are brought in juxtaposition, which induces a pairwise alignment of cells (substep 2.3). Step 3 performs the interaction $\mathcal{I}$ between the aligned cellicules: cells in an aligned pair with equal states do not change state; if they have a different state, they both take the state 0 with probability ν_0, or state 1 with probability $\nu_1 = 1 - \nu_0$. This occurs independently for each aligned pair of cells in the interaction cellicules X, Y, thus producing two identical cellicules (substep 3.1). This "identical twin" replaces the parent cellicules in the population (substep 3.2). Step 4 returns the new population as input to the next iteration of the Algorithm. **(B)**: Metaphorical representation of the algorithm as an artificial chemistry. Eventually, all cellicules get an identical D_3-symmetric configuration.

2.2 Necessity: the ultimate fate caused by the S-algorithm is uniformity in symmetry.

It is clear that populations in which all cellicules have an identical S-symmetric configuration, and only these, are fixed points (equilibrium points) under the operation of the S-algorithm: these populations no longer change as all cellicules are already copies of each other. But this does not mean that this equilibrium state must be reached, as one could

imagine that the random interaction induces permanent random fluctuations in the population. However, having run the S-algorithm for numerous cases, one of which is shown in Figure 3, we are able to formulate the following

Observation 2.1 *The S-algorithm eventually brings all cellicules in an S-symmetric equilibrium state, no matter the population size or the cellicule size.*

This is also illustrated in Figure 2. Note that population size and cellicule size do influence the average number of iterations before the equilibrium is reached. Remark that, if S' is a proper subgroup of the maximal symmetry S of the cellicule's shape, then one could apply the S'-algorithm which ultimately produces S'-symmetric configurations (on an S-symmetric shape).

The algorithm described above has originated from another of our studies [Barbé & von Haeseler, 2003], where a cellular automaton with triangular support was considered, and in which a purposefully designed random feedback enforces its state configuration to become Z_3-symmetric. In the present algorithm, there is no explicit teleological construction.

Fig 13 in Appendix 1 shows a concept of a physical cellicule using bar magnets as cells.

It should be mentioned that the production of mere replicas in artificial chemistries has been reported before [Banzhaf, 1994], [Dittrich *et al.*, 2001]. Here, apart from presenting a new random chemistry which produces replicas, we particularly emphasize the emergence of a symmetric configuration pattern in the replicas.

3 Understanding the algorithm as causing a random walk.

In this Section, we analyze the dynamics of the S-algorithm for $S = Z_1, Z_2, Z_3$. This will give proof for Observation 2.1 for these symmetries. As will be shown later, understanding the algorithm's behaviour for populations of cellicules with S-symmetric shape and with the smallest number of cells, forms the basis for understanding the behaviour in populations of larger-size cellicules. Such so-called *elementary S-cellicules* are displayed in Figure 8(A).

3.1 The population state space and state transition probabilities

Given a cellicule population $\mathcal{P} = \{c_1(n_1), \ldots, c_L(n_L)\}$ of N cellicules (see Eq. (2): n_j is the multiplicity of configuration c_j), the population state is determined by the vector

$$\tilde{\mathsf{z}} = (n_1, n_2, \ldots, n_L) \in \mathbb{N}^L,$$

As it holds that

$$n_1 + n_2 + \ldots + n_L = N,$$

n_L can be considered as a dependent component. It can be removed from $\tilde{\mathsf{z}}$, leaving the state (vector)

$$\mathsf{z} = (n_1, n_2, \ldots, n_{L-1}) \in \mathbb{N}^{L-1}. \tag{4}$$

In what follows, z will be called the *population state*, $\tilde{\mathsf{z}}$ the extended population state. $\mathsf{S}_\mathcal{P}$ denotes the *population state space*, i.e. the set of all population states:

$$\mathsf{S}_\mathcal{P} = \{(n_1, n_2, \ldots, n_{L-1}) | 0 \leq n_1 + n_2 + \ldots + n_{L-1} \leq N\}. \tag{5}$$

If the population state before entering step 2 in an iteration of the S-algorithm is z, it will have changed to a new state z' in step 3.2, before entering the next iteration. This change is induced randomly and makes that the algorithm performs a random walk in the population

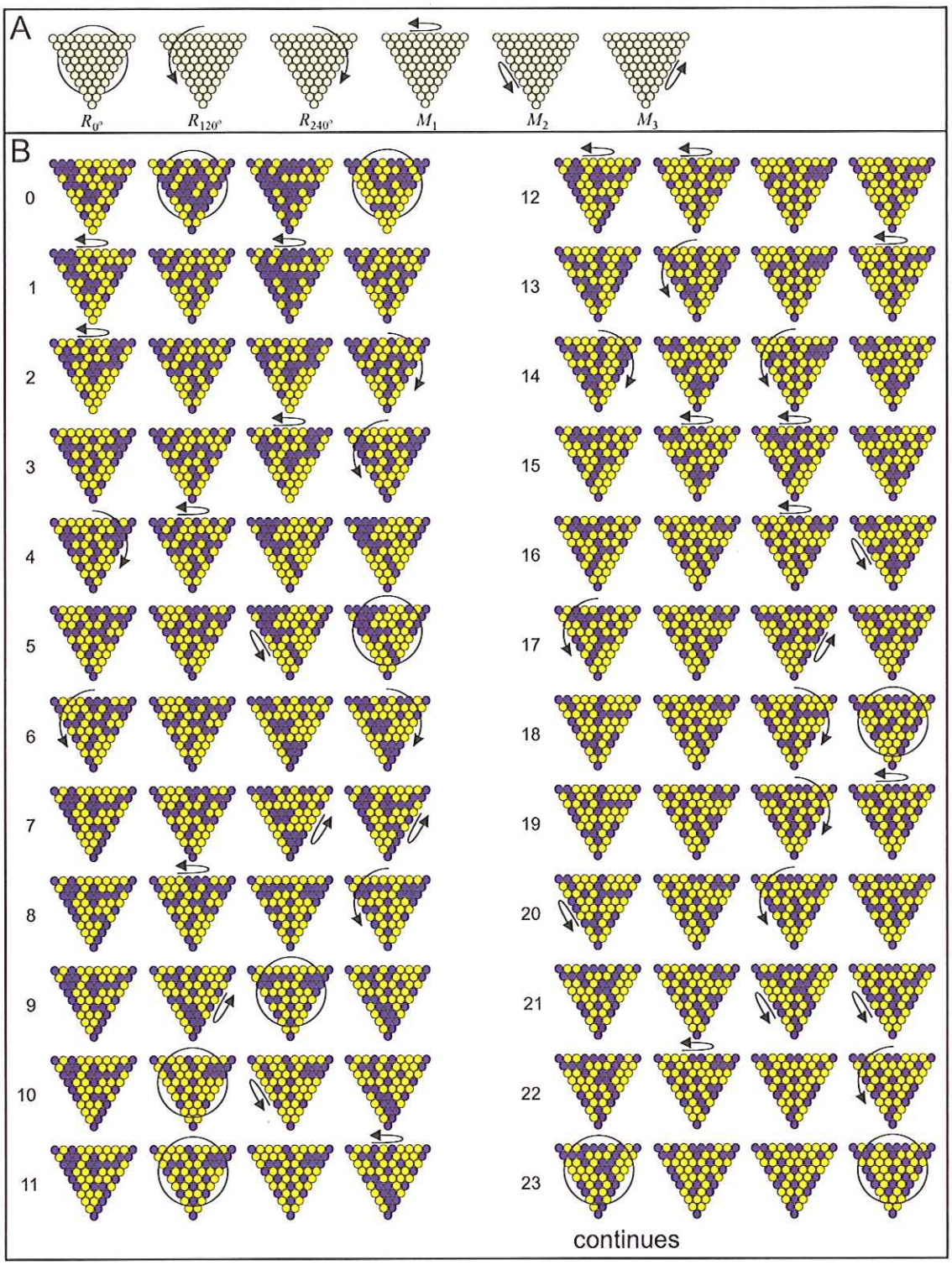


Figure 3: **A**. Marks representing the D_3-operations $R_{0°}$,$R_{120°}$,$R_{240°}$ (= 120°-rotation clockwise). **B**. A possible evolution for a population of 4 triangular cellicules of side-size 10 under the Z_1-algorithm. The numbering concerns the iteration step (0 being the randomly generated initial configuration). At each step k, the two randomly selected cells that will interact to produce the result displayed at $(k+1)$, are marked with the randomly selected reorientations they will undergo before alignment and bilateral random copying (here with $\nu_0 = \nu_1 = 1/2$).

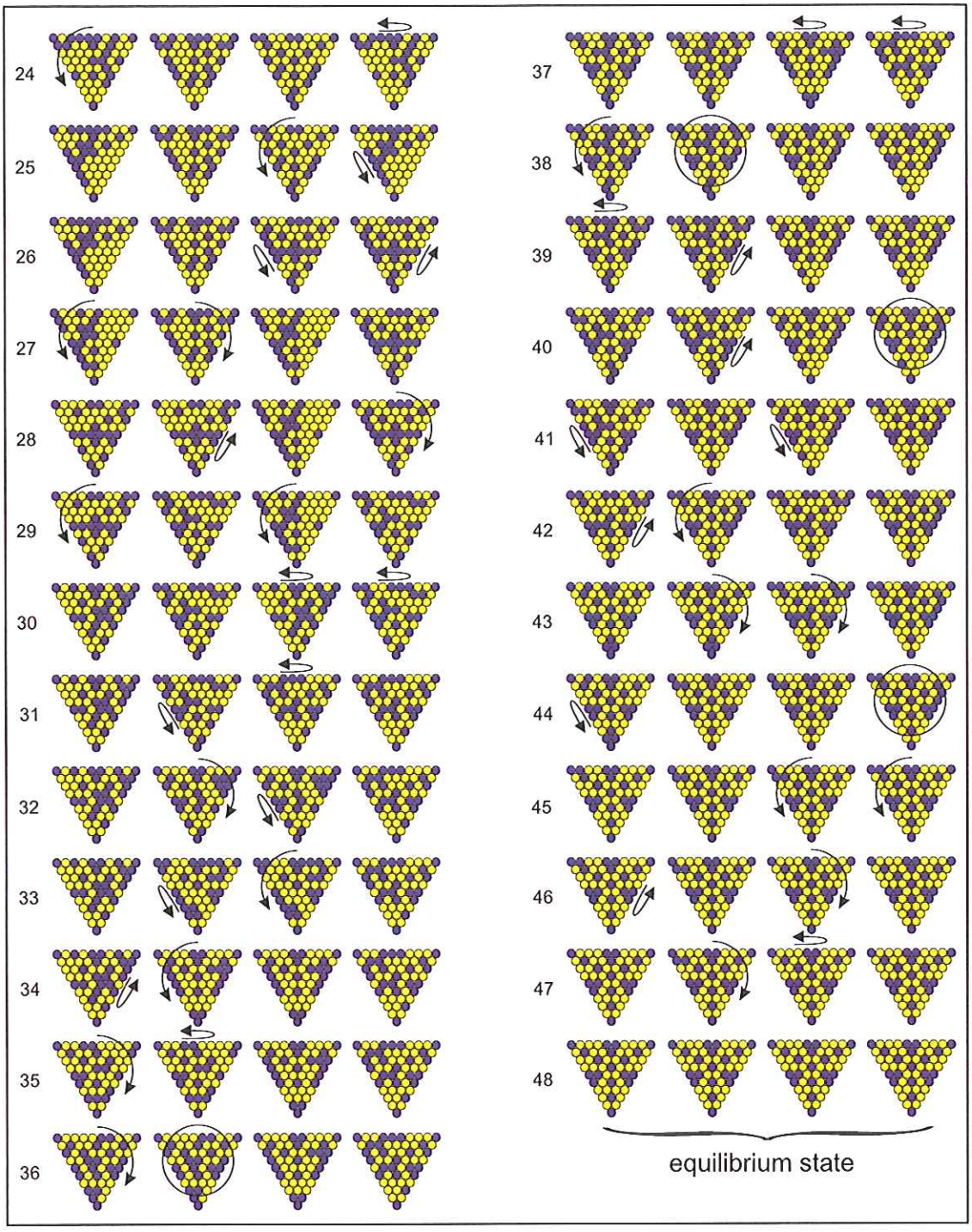


Figure 4: Fig 3 continued.

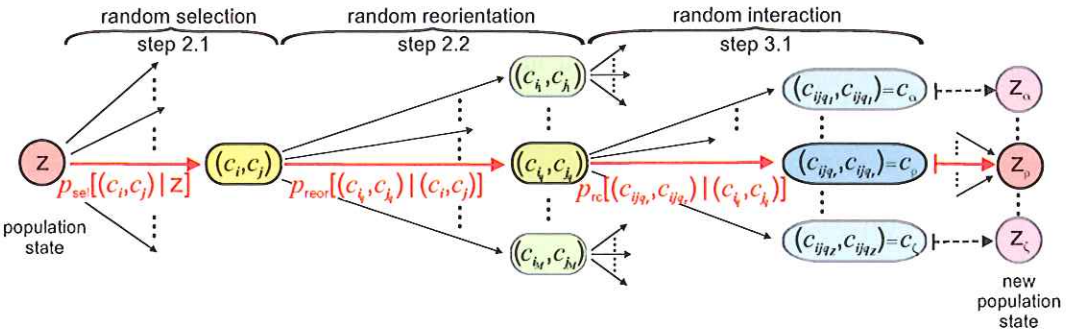


Figure 5: Branches in the probability tree underlying the S-algorithm.

state space. The basis for analyzing the random walk is given by the rooted probability tree structure in Figure 5. It shows how an iteration of the algorithm produces a random transition from a given population state to possible other population states through some branching process. Branches are labelled with the corresponding transition probabilities. At the root of the tree one finds the population state z at the start of step 2. Although step 2.1 randomly selects a cellicule pair, say $C_a, C_b \in \mathcal{P}$, it is not *that* particular choice which determines the further flow of events: any selection of a pair of cellicules with the same configurations as C_a, C_b yields the same possibilities. Hence, for probabilistic analysis, one has to consider in step 2.1 the probabilities of selecting configuration pairs $(c_i, c_j) \in \mathcal{C}^2$, given the population state z. This is denoted

$$p_{\mathsf{sel}}[(c_i, c_j)|\mathsf{z}]. \tag{6}$$

The random reorientations δ_1, δ_2 in step 2.2 of the algorithm transform the selected pair into several possible other pairs (c_{i_q}, c_{j_q}), where $q = 1, \ldots, M(i,j)$ indexes the different outcomes, with respective transition probabilities

$$p_{\mathsf{reor}}[(c_{i_q}, c_{j_q})|(c_i, c_j)]. \tag{7}$$

The fact that all possible reorientations in step 2.2 have equal probability, together with the bilateral symmetry in the subsequent random copying, imply that no distinction has to be made between (c_i, c_j) and (c_j, c_i). In that sense, it is better to consider in Eqs.(6,7) configuration pairs which are member of the **rest**ricted set

$$\mathcal{C}^2_{\mathsf{rest}} = \{(c_i, c_j)|(c_i, c_j) \in \mathcal{C}^2,\ i \leq j\}.$$

In step 3.1, each possible reoriented pair (c_{i_q}, c_{j_q}) interacts by bilateral random copying, and produces a pair of identical cellicules with configuration $c_{ijq_r} = R(c_{i_q}, c_{j_q}) \in \mathcal{C}$. r indexes the different possibilities and ranges from 1 to $Z(i,j,q)$. The corresponding "random copying" transition probability is denoted

$$p_{\mathsf{rc}}[(c_{ijq_r}, c_{ijq_r})|(c_{i_q}, c_{j_q})]. \tag{8}$$

In step 3.2, the replacement of the interacting cellicules by their interaction product $c_{ijq_r} = c_\rho \in \mathcal{C}$ changes the population state z into z′, in a unique way which depends on z and c_ρ, as follows:

- A. case $i \neq j$, i.e., the selected parent cellicules at step 2.1 have different state configurations

-(a) when $\rho \neq i, j$, i.e., the interaction products differ from the interacting cellicules,

$$\tilde{\mathsf{z}} = (n_1, \ldots, n_i, \ldots, n_j, \ldots, n_\rho, \ldots, n_L\} \rightarrow \tilde{\mathsf{z}}' = (n_1, \ldots, n_i{-}1, \ldots, n_j{-}1, \ldots, n_\rho{+}2, \ldots, n_L)$$

(The extended state $\tilde{\mathsf{z}}$ is used because i, j, ρ may equal L. The corresponding state z is obtained by deleting the last component in $\tilde{\mathsf{z}}$. Note also that a transfer is only possible when both z and $\mathsf{z}' \in \mathsf{S}_{\mathcal{P}}$).

-(b) when $\rho = i$ (similar in case $\rho = j$), i.e., the interaction products are the same as one of the interacting cellicules,

$$\tilde{\mathsf{z}} = (n_1, \ldots, n_i, \ldots, n_j, \ldots, n_L) \rightarrow \tilde{\mathsf{z}}' = (n_1, \ldots, n_i + 1, \ldots, n_j - 1, \ldots, n_L)$$

- B. case $i = j$, i.e., the selected parent cellicules at step 2.1 have the same configuration

-(a) when $\rho \neq i$, i.e., the interaction product differs from the interacting cellicules,

$$\tilde{\mathsf{z}} = (n_1, \ldots, n_i, \ldots, n_\rho, \ldots, n_L) \rightarrow \tilde{\mathsf{z}}' = (n_1, \ldots, n_i - 2, \ldots, \ldots, n_\rho + 2, \ldots, n_L).$$

-(b) when $\rho = i$, i.e., the interaction product is the same as the interacting cellicules,

$$\tilde{\mathsf{z}} = (n_1, \ldots, n_i, \ldots, n_L) \rightarrow \tilde{\mathsf{z}}' = \tilde{\mathsf{z}}$$

In general, it is possible that a particular state z can be transformed into another particular state z' via distinct paths (paths are distinct if they have at least one uncommon branch).

All *branch probabilities* (6,7,8) can be calculated in principle. A certain path connecting the root with one of the end nodes in the tree has a *path probability* which is the product of the probabilities that label the branches of the path, and is of the form

$$p_{\mathsf{sel}}[(c_i, c_j)|\mathsf{z}]p_{\mathsf{reor}}[(c_{i_q}, c_{j_q})|(c_i, c_j)]p_{\mathsf{rc}}[(c_\rho, c_\rho)|(c_{i_q}, c_{j_q})].$$

From the structure of the tree, it then follows that the transition probability $p(\mathsf{z}'|\mathsf{z})$ is given by the sum of the path probabilities over all distinct paths connecting z to z':

$$p(\mathsf{z}'|\mathsf{z}) = \sum_{\substack{\text{over all distinct paths} \\ \mathsf{z} \rightarrow \mathsf{z}'}} p_{\mathsf{rc}}[(c_\rho, c_\rho)|(c'', c''')]p_{\mathsf{reor}}[(c'', c''')|(c, c')]p_{\mathsf{sel}}[(c, c')|\mathsf{z}]. \qquad (9)$$

These probabilities define a Markov chain transition probability matrix and induce a random walk in the population state space. We will show next, for populations of cellicules subject to the Z_1-,Z_2-,and Z_3-algorithm, that this random walk ends by absorption in an equilibrium state where the population consists of identical symmetric cellicules.

3.2 Population dynamics under the Z_1-Algorithm

3.2.1 Dynamics in a population of single-cell cellicules under the Z_1-algorithm

Consider the simplest case: a population of N single-cell cellicules. The set of cellicule configurations in this case is $\mathcal{C} = \{0, 1\}$. Let z_0 denote the number of cellicules with configuration 0 in the population, and $z_1 = N - z_0$ the number of cellicules with configuration 1. Then the population state is z_0, and the population state space, denoted $P_{N,1}$, is $P_{N,1} = \{z_0 | 0 \leq z_0 \leq N\} = \{0, 1, \ldots, N\}$. (The 1 in the subscript of $P_{N,1}$ refers to the number of cells in the cellicule. Later we will also consider $P_{N,n}, n \neq 1$.)

Theorem 3.1 *The Z_1-algorithm brings all N single-cell cellicules into an identical configuration state, with a probability that tends to 1 as the number of iterations tends to infinity.*

Proof: Let $z_0(k-1)$ denote the population state before the algorithm enters the k-th iteration of step 2. After step 3 in the k-th iteration, the population state gets updated to $z_0(k)$ in a random way provided by the random pair selection step 2.1 and the random copying step 3.1. We derive the transition probability

$$p(x|z) = p[z_0(k) = x | z_0(k-1) = z]$$

using Eq.(9), after construction of the probability tree. Hereby we take into account that the reorientation step can be considered void because the only possible reorientation is the identity, which removes the random reorientation branches in the general tree structure of Fig. 5. The possible configuration pairs that may occur as outcomes of the random selection step 2.1 form the set $\mathcal{C}^2_{\mathsf{rest}} = \{(0,0),(0,1),(1,1)\}$. Here follows the analysis for these three possibilities:

(a) Selection $(0,1)$ has probability

$$p_{\mathsf{sel}}[(0,1)|z] = \frac{z(N-z)}{\binom{N}{2}} = \frac{2z(N-z)}{N(N-1)}. \tag{10}$$

(the number of possible choices for selecting a cellicule in state 0 or 1 being z and $(N-z)$ respectively, and $\binom{N}{2}$ being the number of all possible selections of 2 cellicules out of N). The subsequent random copying results in

(a1) the cellicule pair $(0,0)$, with probability $p_{\mathsf{rc}}[(0,0)|(0,1)] = \nu_0$. This induces the population state transition $z \to z+1$, with path probability $\nu_0 p_{\mathsf{sel}}[(0,1)|z]$

(a2) the cellicule pair $(1,1)$, with probability $p_{\mathsf{rc}}[(1,1)|(0,1)] = \nu_1$. This induces the population state transition $z \to z-1$, with path probability $\nu_1 p_{\mathsf{sel}}[(0,1)|z]$.

(b) Selection $(0,0)$ has probability

$$p_{\mathsf{sel}}[(0,0)|z] = \binom{z}{2} \Big/ \binom{N}{2} = \frac{z(z-1)}{N(N-1)} \tag{11}$$

($\binom{z}{2}$ being the number of possible choices for selecting two cellicules in state 0). The subsequent random copying can only produce the pair $(0,0)$. Thus the corresponding transition probability $p_{\mathsf{rc}}[(0,0)|(0,0)] = 1$. This interaction does not change the population state and produces the transition $z \to z$, with corresponding path probability $p_{\mathsf{sel}}[(0,0)|z]$.

(c) Selection $(1,1)$ has probability

$$p_{\mathsf{sel}}[(1,1)|z] = \binom{N-z}{2} \Big/ \binom{N}{2} = \frac{(N-z)(N-z-1)}{N(N-1)} \tag{12}$$

Then $p_{\mathsf{rc}}[(1,1)|(1,1)] = 1$ and again this will not change the population state. It results in a transition $z \to z$, with corresponding path probability $p_{\mathsf{sel}}[(1,1)|z]$.

The corresponding probability tree is given in Figure 6.

Using (9), this gives the overall transition probabilities

$$p(z+1|z) \stackrel{\mathsf{def}}{=} p_z = \frac{2\nu_0 z(N-z)}{N(N-1)} \tag{13}$$

$$p(z-1|z) \stackrel{\mathsf{def}}{=} q_z = \frac{2\nu_1 z(N-z)}{N(N-1)} \tag{14}$$

$$p(z|z) \stackrel{\mathsf{def}}{=} r_z = 1 - \frac{2z(N-z)}{N(N-1)} \text{ (summing path probabilities of (b) and (c))} \tag{15}$$

$$p(x|z) = 0 \text{ when } x \neq z, z+1, z-1. \tag{16}$$

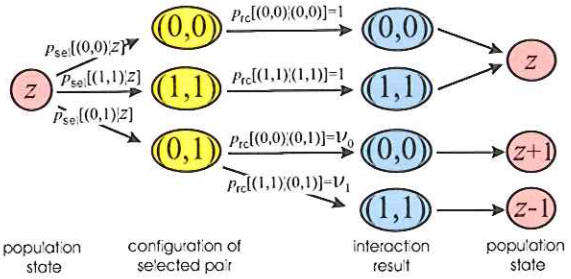


Figure 6: The complete probability tree underlying the evolution of a population of single-cell cellicules.

Observe that, of course, $p_z + q_z + r_z = 1$. It is clear that a transition given in this general form only makes sense in case both states appearing in it belong to the state space $P_{N,1} = \{0, 1, \ldots, N\}$. E.g., when $z = 0$ the transition $z \to z - 1$ (i.e. $0 \to -1$) does not exist, while the transition $z \to z + 1$ (i.e. $0 \to 1$) has probability $p_0 = 0$. But there is consistency with the formulae also in the first case, as the calculated probability for the nonexisting event is also 0 (cf. Eq.(14)).

All the above shows that the population state z_0 evolves as a Markov chain on the state space $\{0, 1, \ldots, N\}$, with the following state transition probability matrix $P = P(i,j)_{i,j\in\{0,1,\ldots,N\}}$ where $P(i,j) = p(j|i)$:

$$P = \begin{bmatrix} 1 & 0 & 0 & 0 & 0 & \cdots & 0 & 0 & 0 & 0 & 0 \\ q_1 & r_1 & p_1 & 0 & 0 & \cdots & 0 & 0 & 0 & 0 & 0 \\ 0 & q_2 & r_2 & p_2 & 0 & \cdots & 0 & 0 & 0 & 0 & 0 \\ \vdots & & & & \vdots & \ddots & \vdots & & & & \vdots \\ 0 & 0 & 0 & 0 & 0 & \cdots & 0 & q_{N-2} & r_{N-2} & p_{N-2} & 0 \\ 0 & 0 & 0 & 0 & 0 & \cdots & 0 & 0 & q_{N-1} & r_{N-1} & p_{N-1} \\ 0 & 0 & 0 & 0 & 0 & \cdots & 0 & 0 & 0 & 0 & 1 \end{bmatrix} \tag{17}$$

This Markov process actually corresponds to the gambler's ruin random walk, as for example described in [Parzen, 1967] Example 6A, Eq.(6.24). It has absorbing states $z = 0$ and $z = N$ (corresponding to populations where all cellicules are in state 1 or state 0 respectively). All other population states $1, 2, \ldots, N-1$ are nonrecurrent (transient). It means that, no matter the initial value of the population state z_0, the population state will get into one of the two absorbing states. This will happen with a probability tending exponentially to 1 as the number of iterations increases [Kemeny & Snell, 1976].

■

As recalled in Appendix 2, knowledge of the transition probability matrix P allows to determine the probabilities $f_{z\to 0}$ and $f_{z\to N}$ for being absorbed into states 0 and N respectively, when starting with a population in state z. Also $m(z)$, the average number of iterations before absorption when starting in state z, can be calculated. Figure 7 summarizes a few results concerning these quantities. They will be helpful in the discussion (Sec. 4).

3.2.2 Dynamics in a population of multicell cellicules under the Z_1-Algorithm

Now consider a population of N cellicules of size n, subject to the Z_1-algorithm. Clearly, the random copying interactions only occur between cells taking the same position in

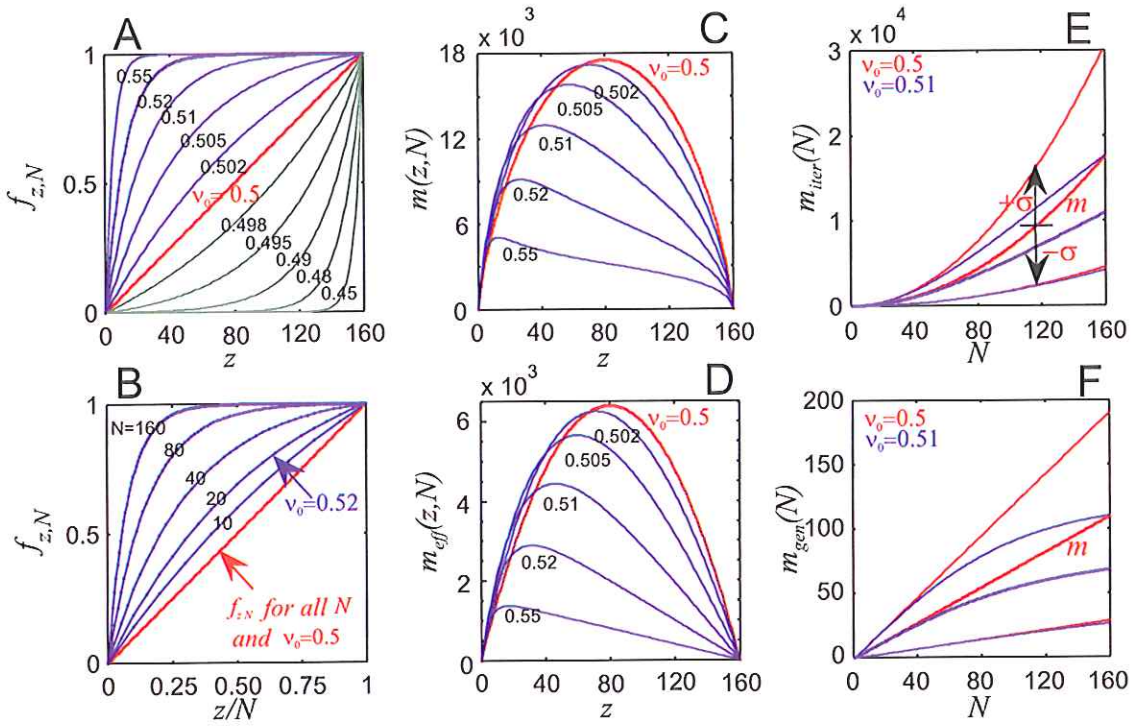


Figure 7: Results for a population of N single-cell cellicules ($N = 160$). z is the initial number of cellicules in the population with configuration state 0. A: The probability $f_{z,N}$ of absorption in population state N (all cellicules having configuration state 0), as a function of z, for distinct values of ν_0. The probability $f_{z,0}$ for absorption in state 0 (all cellicules are in state 1) is complementary ($f_{z,0} = 1 - f_{z,N}$). B: the absorption probability $f_{z,N}$ for a fixed value of $\nu_0 \neq 0.5$ (here $\nu_0 = 0.52$) increases with increasing N for a given ratio z/N. For $\nu_0 = 0.5$, this absorption probability is independent of the population size. C: the average number $m(z,N)$ of iterations in the Z_1-algorithm before absorption in one of the equilibrium population states 0 or N, as a function of the initial state z ($N = 160$). This average number decreases for increasing distance of $\nu_0 > 0.5$. (For values $\nu_0 < 0.5$, the curve is the left-right reflection of the corresponding curve for $1 - \nu_0$). D: the average number $m_{\text{eff}}(z,N)$ of effective iterations (producing cellicule interactions that effectively change the population state) before absorption. Comparison with figure C shows that this average is roughly three times smaller than for the total count of iterations. E: the average number m_{iter} of iterations (denoted m) before absorption as a function of the population size, together with the spread ($m \pm \sigma$, σ being the standard deviation), for $\nu_0 = 0.5$ and $\nu_0 = 0.51$ (red and blue curves respectively). The average is based on the assumption that each cell in the population is given a state 0 or 1 independently, according to a fair coin tossing experiment. F: like figure E, but now displaying $m_{\text{gen}}(N) = m_{\text{iter}}(N)/N$, which can be interpreted as the average number of generations before absorption, a generation corresponding to a number of iterations after which on average each cellicule has partaken in an interaction. It gives an idea about the number of iterations in case the algorithm iterates pairs of cellicules in parallel (as would be the case in real chemical reactions). Notice the linear character of $m_{\text{gen}}(N)$ when $\nu_0 = 0.5$.

the cellicules, and not between cells in different positions. This is illustrated in Figure 8B(left) for rectilinear string-cellicules, where cells in the same position are confined to a "column" under proper cellicule alignment. Together with the fact that a random selection of cellicules also provides a random selection of cells in any particular column, this implies that the evolution of the cells in any isolated column is the same as that of a population of N single-cell cellicules studied above. As a consequence, all cells in a column will eventually reach the same state 0 or 1. Looking at the global picture, one sees that there is a column where all cells get into the same state first (the corresponding random walk in the population state space of that column reaches one of its absorbing states). Then the algorithm actually continues performing on a population of N cellicules of size $(n-1)$. Again, after some time, all cells in one of the remaining columns will reach the same state and do no longer change. This reduces again the effective size of the cellicules by one. And this reduction continues, until all columns show their cells in an identical state (the state may differ from column to column). In conclusion, we can formulate

Theorem 3.2 *The Z_1-algorithm brings all cellicules in the population into an identical Z_1-symmetric configuration (with a probability tending to 1 with increasing number of iterations, and no matter the cellicule size or the population size).*

The process just described is a random walk which generally starts inside the associated (2^n-1)-dimensional population state polyhedron $P_{N,n}$ (see Appendix 4), and enters random walks of ever reducing dimension. The full description of the random walk needs the determination of the associated probability transition matrix of states in $P_{N,n}$, from which also the absorption probabilities and average absorption times can be calculated. This probability transition matrix cannot be modelled properly by a product of one-dimensional random walks because the selection of interacting cells in different columns are not independent (they belong to the same randomly selected cellicules). The determination of the transition probability matrix becomes quickly infeasible for growing cellicule size, because of the huge dimensionality involved. However, it is still feasible and very instructive to analyze the case for a population of N two-cell cellicules subject to the Z_1-algorithm. This also prepares for the study of the Z_2- and Z_3-case. We formulate here the main conclusions of this analysis.

3.2.3 Dynamics in a population of 2-cell cellicules under the Z_1-Algorithm

Let ab, $a,b,\in\{0,1\}$ denote the configuration of a two-cell string-cellicule where the first (leftmost) cell has state a and the second cell has state b. Let z_{ab} denote the number of cellicules in the population with configuration ab. As the total population contains N cellicules, it holds that $z_{00}+z_{01}+z_{10}+z_{11}=N$. The population state is defined by the vector (z_{00},z_{01},z_{10}), constrained by the condition $z_{00}+z_{01}+z_{10}\leq N$, and the population state space $P_{N,2}$ is the set of all points in $\mathbb{N}^3$ confined by the tetrahedron OABC, as illustrated in Figure 14 (Appendix 5). The analysis in Appendix 5 shows that the possible state transitions in $P_{N,2}$ define a random walk with four absorbing states $(N,0,0)$, $(0,N,0)$, $(0,0,N)$, $(0,0,0)$. These correspond to populations where all cellicules have configurations 00, 01, 10, 11 respectively. All other states are transient.

Compartment (b,IV) in Figure 9 repeats the structure of $P_{N,2}$ in an overview table which allows it to compare to several other elementary Z_1-,Z_2-,Z_3-cases (some of which remain to be discussed further). Figure 9(b,V) shows the probability of being absorbed in the equilibrium point A when starting from a given initial state $z\in P_{N,2}$. Figure 9(b,VI) displays the average number of iterations m_z before reaching an equilibrium state when starting from a given initial state z. These have been calculated using the fundamen-

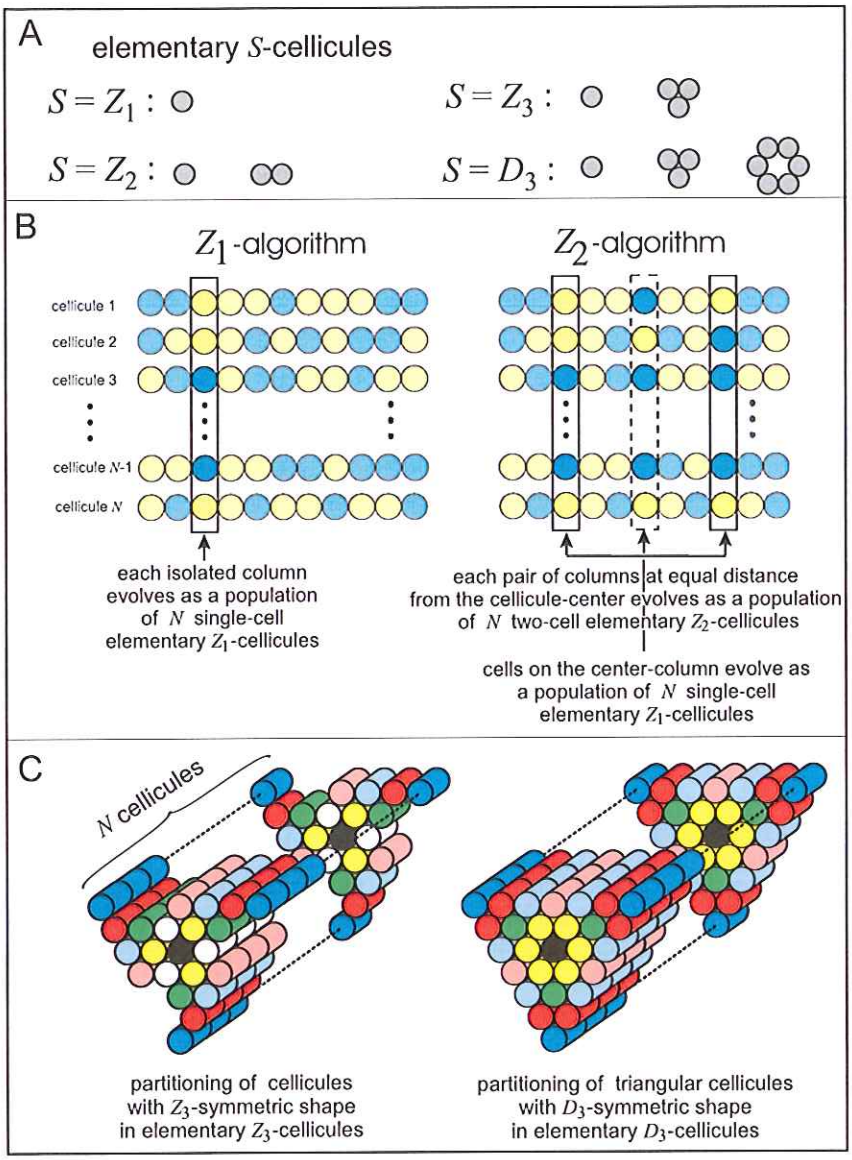


Figure 8: **(A)** Elementary cellicules with Z_1-,Z_2-,Z_3-,and D_3-symmetric shape. **(B)** Left: partitioning of Z_1-symmetric string-cellicules of arbitrary size into elementary Z_1-cellicules. Right: partitioning of Z_2-symmetric string-cellicules of arbitrary size into elementary Z_2-cellicules. **(C)** Partitioning of Z_3- and D_3-symmetric cellicules in elementary Z_3- and D_3-cellicules. Each distinct elementary cellicule has its own colour.

tal matrix method explained in Appendix 2.2, and based on the transition probabilities derived in Appendix 5.

Notice that, although the cells at a particular position in these two-cell cellicules, when observed in isolation ("columnwise", see above), perform a one-dimensional random walk, they do not so independently. That is the reason why the state space $P_{N,2}$ is not the product $\hat{P}_{N,2}$ of two $P_{N,1}$ spaces (a detailed analysis of the state transitions in $\hat{P}_{N,2}$ is given in Appendix 6, and the corresponding graphs are displayed in Figure 9(d)). Nevertheless,

a relevant observation from the numerical calculations is that absorbing probabilities in $P_{N,2}$ can be obtained from the products of corresponding absorbing probabilities in $P_{N,1}$. For example, the absorption probability $f_{(z_{00},z_{01},z_{10})\to(0,N,0)}$ in $P_{N,2}$ satisfies

$$f_{(z_{00},z_{01},z_{10})\to(0,N,0)} = f_{z_0\to 0} f_{z_0'\to N},$$

where $z_0 = z_{00} + z_{01}$ and $z_0' = z_{00} + z_{10}$, and $f_{z_0\to 0}$ and $f_{z_0'\to N}$ are absorption probabilities for the one-dimensional random walk in $P_{N,1}$. (Figure 9(d,V) displays $f_{(z_0,z_0')\to(N,N)} = f_{z_0\to N} f_{z_0'\to N}$in $\hat{P}_{N,2}$, which equals $f_{(z_{00},z_{01},z_{10})\to(N,0,0)}$ in $P_{N,2}$). This observation is made plausible by the fact that the cells at any of the two positions in the cellicules, when looked upon separately, evolve as a one-dimensional random walk for which the absorbing probability only depends on the initial state (number of cells in state 0) in that position. Clearly, the number of 0-state cells in the first position is given by $z_0 = z_{00} + z_{01}$, in the second position by $z_0' = z_{00} + z_{10}$. We **conjecture** (a rigorous proof still lacking) that this **absorption probability product-property** also holds for the absorbing probabilities of larger-size cellicules. This apparent independency induced by the *partitionability* of the cellicules into single-cell cellicules does not hold for the average number of iterations before absorption. However, numerical evaluations indicate that this average for a population of N two-cell cellicules, when the cells in the cellicules are initialized randomly and independently, is *approximately* the same as the average number of iterations needed to bring two independent populations of N single-cell cellicules in their equilibrium state. It is tempting to conjecture that this approximation extends to larger-size cellicules evolving under the Z_1-algorithm.

3.3 Dynamics under the Z_2-algorithm

The right part of Fig. 8B illustrates that the partitionability argument also works for the Z_2-algorithm acting on multicell string-cellicules: the dynamics is explained by the algorithm's action on two-cell elementary Z_2-cellicules. Indeed, the random interactions occur exclusively between cells in "columns" which are placed at the same distance from the center of the cellicule. Thus, the population of cellicules can always be partitioned into such "bi-columns" of elementary Z_2-cellicules. Figure 2B shows a case where also a population of single-cell cellicules has to be considered in this partitioning. But the Z_2-dynamics on this simplify to the already analyzed Z_1-dynamics.

The analysis for the evolution of a population of N two-cell cellicules under the Z_2-algorithm (see Appendix 7) shows the that population state space remains $P_{N,2}$. However, the possible transitions under the Z_2-algorithm now define a two-dimensional random walk with only two absorbing states $(0,0,0)$ and $(N,0,0)$, while all other states are transient. As a consequence, the Z_2-algorithm will ultimately bring all cellicules in a population of two-cell cellicules into an identical configuration state 11 or 00. Together with the abovementioned partitioning argument, this leads to the following statement concerning a population of N cellicules of size N with Z_2-symmetric shape:

Theorem 3.3 *The Z_2-algorithm brings all cellicules in the population into an identical Z_2-symmetric configuration (with a probability tending to 1 with increasing number of iterations, and no matter the cellicule size or population size).*

Results for the two-cell cellicule case evolving under the Z_2-algorithm concerning the probability of reaching the particular equilibrium state $(N,0,0)$ from a given initial population state, and the average number of iterations until absorption, are shown in Figure 9(c,V-VI).

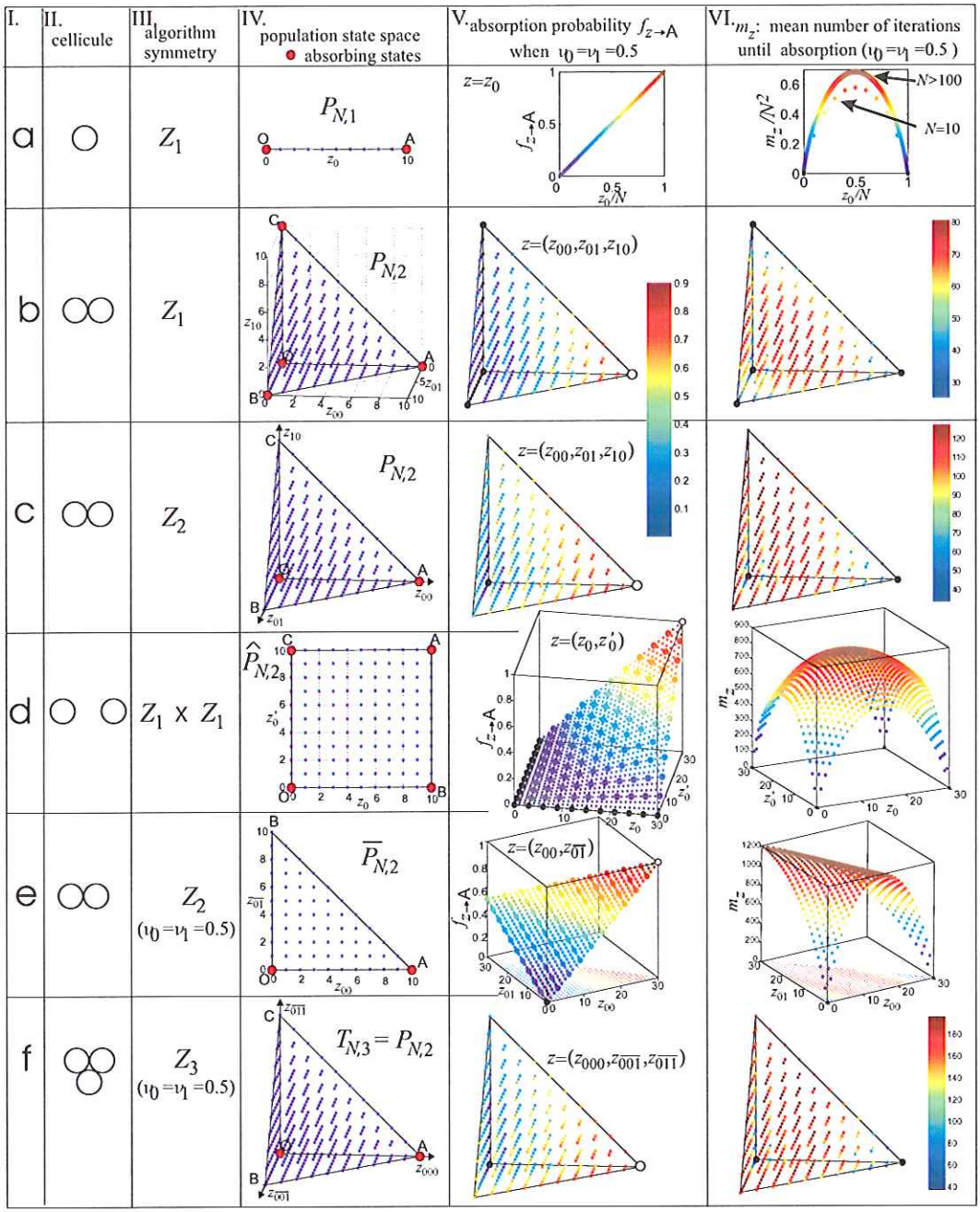


Figure 9: Column IV shows the population state spaces for populations of elementary cellicules (displayed in column II), and acted upon by the S-algorithm (S mentioned in column III). The population size $N = 10$. States displayed in red are the absorbing (equilibrium) states. The population state spaces are identical for **b**,**c**,**f**, but the random walk induced by the corresponding S-algorithm differs. In some of the higher dimensional spaces, there are absorbing one-dimensional random walks: for **b** on OC,OB,CA,AB; for **d** on OC, OB, CA, AB. Column V displays the absorption probability $f_{z\to A}$ for going from state z in the population state space to absorbing state A under the unbiased random copying condition $\nu_0 = \nu_1 = 0.5$. The value of $f_{z\to A}$ is colorcoded, and for **d**,**e**, it is also displayed as the vertical coordinate value. The closer z is to A, the higher the probability of being absorbed by A. The absorption probabilities for other equilibrium states give an identical picture under proper reorientation of the tetrahedron OABC. Column VI shows m_z, the average number of iterations before absorption in one of the equilibrium states, when starting from an initial state z (also under the condition $\nu_0 = \nu_1 = 0.5$). Starting closer to a particular equilibrium state will on average require less iteration steps to reach an equilibrium state (with high probability this will be that particular equilibrium state). The images remain qualitatively similar for other population sizes N. For the absorption probabilities in column V, the pictures also remain qualitatively invariant under renormalization $z \to z/N$, just like for the case under **a**. This is made clear in **d**,**e**, where values are shown for $N = 10$ (the "fat" dots) and $N = 30$ (the "thin" dots). The mean number of iterations m_z in column VI tends to grow quadratically with N for constant z/N (similar to the case under **a**).

A next observation is that, for the Z_2-algorithm acting on a population of two-cell cellicules, it is possible to identify the cellicule configurations 01 and 10 into one equivalence class denoted $\overline{01}$ (see Appendix 7 for details). The population state is then the lumped state $(z_{00}, z_{\overline{01}})$ with $z_{00} + z_{\overline{01}} \leq N$ (and $z_{00} + z_{\overline{01}} + z_{11} = N$). The corresponding two-dimensional state space $\overline{P}_{N,2}$, and related aborption probability and average number of iterations before absorption, are shown in Figure 9(e, IV-VI). It is exactly this strategy of incorporating the reorientation symmetry of the algorithm in the definition of equivalence classes for the configuration states, which makes it still feasible to give proof for the behaviour of the Z_3-algorithm applied to elementary Z_3-cellicules.

3.4 Dynamics under the Z_3-algorithm

If the distinct cells in a three-cell elementary Z_3-cellicule (see Figure 8A) are denoted $c(1)$,$c(2)$,$c(3)$, then abc, $a, b, c \in \{0, 1\}$ denotes the configuration in which the states of $c(1), c(2), c(3)$ are a, b, c respectively. The configuration classes modulo Z_3 are then 000, $\overline{001} = \{001, 010, 100\}$, $\overline{011} = \{011, 110, 101\}$, and 111 (whereby the classes with a single configuration are denoted by that single configuration, without overline). With z_{abc} denoting the number of cellicules in the population having configuration abc, the population state space $T_{N,3}$ is defined by the vectors $(z_{000}, z_{\overline{001}}, z_{\overline{011}})$ with the condition $z_{000} + z_{\overline{001}} + z_{\overline{011}} \leq N$. Actually $T_{N,3} = P_{N,2}$ (see Fig. 8(f,IV)), but the possible transitions and their probabilities in $T_{N,3}$ differ from what is the case in $P_{N,2}$ for Z_1- and Z_2-symmetries. See Appendix 8 for the complete analysis. Here again, there are four absorbing states which correspond to the equilibrium states where all cellicules in the population have either the configuration 000, $\overline{001}$, $\overline{011}$, or 111. Figure 8(C)(left) refers again to the partitioning argument and shows that a population of cellicules with Z_3-symmetric shape evolves along disjoint elementary Z_3-cellicules (and possibly a single-cell cellicule in the center) under the Z_3-algorithm. As a consequence, we can formulate

Theorem 3.4 *The Z_3-algorithm brings all cellicules in the population into an identical Z_3-symmetric configuration (with a probability tending to 1 with increasing number of iterations, no matter the cellicule size or population size).*

3.5 Dynamics under general S-symmetry

The analysis reported above shows the way to tackle the evolution in a population of cellicules with a more general symmetry S: only the evolution of populations of elementary S-cellicules has to be established. These elementary cellicules are shown in Figure 8A for $S = D_3$, and may consist of one, three or six cells. Figure 8C (right) shows how a D_3-symmetric cellicule is partitioned in elementary D_3-cellicules. However, the growing dimensionality quickly limits the feasibility of analyzing populations of elementary cellicules. For example, for the six-cell elementary D_3-cellicule, even when considering compacted population states (by reducing D_3-symmetric state configuration modulo D_3), one needs to take into account 16 configuration classes, yielding a 15-dimensional population state space, and 136 possible class-interactions. Despite the impracticability of analyzing this case, the analysis for the simpler cases presented in this paper and the experimental evidence corroborate the conjecture that the S-algorithm for more general S-symmetries will ultimately lead to an equilibrium state where all cellicules have the same S-symmetric configuration. Providing a general proof about the "random walk with absorbing states"-character of the dynamics, which is valid for all S, remains a challenge.

4 Discussion: Mixing species, mutations, variations on the algorithm

The S-algorithm illustrates how random interactions on a microscopic level (the cellwise random copying), combined with a random exploitation of "low level" symmetry (the geometrical/physical symmetry of the cellicule shape) brings the symmetry to the "high level" of the cellicules' configuration. All interacting cellicules ultimately become replicas of each other. Having an abundant number of replicas of interacting subjects is the key-precondition for evolution under mutation. A random mutation in one or more cellicule configurations in an equilibrium population can initiate a possible change in the whole population. Also, letting the algorithm act on parts of a population which become separated (or on different populations of the same type of cellicules) will generate different "species". We will discuss a few evolutionary experiments in more detail.

4.1 Populations of single-cell cellicules: a sociodynamical metaphor

Consider two populations of single-cell cellicules that have evolved separately to their equilibrium state under the Z_1-algorithm. One population has N_A members which all hold a conviction (opinion, taste, belief, mood...) A, and the other has N_B members holding conviction B. Then these populations are brought together and mix through recurrent contacts between two individuals. Contact between members with the same conviction changes nothing. After contact between two individuals with distinct conviction, one individual converts by copying the conviction of the other: with probability ν_A both individuals will have conviction A after the encounter, and with probability $\nu_B = 1 - \nu_A$ both will have conviction B. Associating conviction A with state 0, and B with state 1, this situation corresponds to a population of $N = N_A + N_B$ single-cell cellicules described above, with an initial state $z = N_A$, and evolving under the Z_1-algorithm. It follows that ultimately all individuals will get the same conviction, either A or B (the average number of contacts needed for this to happen depends on z, see Figure7(C,D)). We refer to Figure 7)(A) for what follows. In the unbiased case $\nu_A = \nu_B = 0.5$, which reflects an equal "convincing power" for both convictions, the probability that all will eventually get conviction A exceeds 0.5 when the A-population is initially in the majority: it is as if the majority provides an intrinsic "conviction pressure". This majority-pressure can be countered by increasing the convincing power of B, by letting $\nu_B > \nu_A$. But one thing is clear: the ultimate fate is uniformity. Disabling interactions is the only way to preserve diversity. A superficial complication could arise when considering a more realistic model in which, upon encounter of two individuals with distinct convictions, an individual with conviction A converts with probability $\nu_{A\to B}$ to B and keeps its own conviction with probability $\nu_{A\to A} = 1 - \nu_{A\to B}$, while (at the same occasion) the other individual B converts to A with probability $\nu_{B\to A}$(and keeps its own conviction with probability $\nu_{B\to B} = 1-\nu_{B\to A}$. This case of "autonomous change of conviction" is essentially equivalent with the original one through a proper parameter change (see Appendix 9). But here the impossibility of a single conviction, say A, to change (i.e. $\nu_{A\to B} = 0$), while members of the other conviction are allowed to change, will convert all individuals to A. If both convictions are forbidden to change ($\nu_{A\to B} = 0$ and $\nu_{B\to A} = 0$), then the initial population state remains status quo.

Of course, we have to be careful with such a metaphor. Using the words "individuals" and "conviction/opinion" may suggest that some "conscious" action is involved. The Z_1-algorithm does not suggest this, but it is not excluded either. Exactly this makes the example more than a metaphor: whether there is consciousness, threatening, sociologi-

cal/psychological pressure, susceptibility to rational or irrational convictions involved or not: it's all present (hidden) in the statistics via the parameters ν_A, ν_B. Figure 7)(A) even allows to follow the probabilities for being attracted to either conviction in case these parameters would change. In connection with this, we ran several experiments where the copying probability ν_0 in step 3.1 of the algorithm changes randomly at each iteration. This leads to a nonhomogeneous form of the random walk, where the transition probability matrix (17) changes at each iteration by letting ν_0 and $\nu_1 = 1 - \nu_0$ change accordingly in (13)-(14). Figure 10 shows how the absorption probability $f_{z\to N}(N = 59, z = 30)$ evolves as the number of iterations grows when ν_0 is selected randomly and independently at each iteration according to the uniform distribution in $[0, 1]$. The result is clear: also here, the population is attracted to an equilibrium state where all cells have the same state. The only difference is that $f_{z\to N}$ varies over different runs of the experiment (and has become a random variable in itself). $f_{z\to N}$ is obtained as the limit $p(N|z) = \lim_{M\to\infty} P(M)P(M-1)\dots P(1)p_0(z)$, where $P(k)$ is the transition probability matrix (17) at the k-th iteration step, and $p_0(z)$ is the initial state probability vector $(p_0(i))_{i=0,1,\dots N}$ with $p_0(z) = 1$ and all other components equal to zero. Possibly, the same fate of ultimate uniformity will occur when ν_0 changes along the iterations in another way, randomly or not: it might just change the absorption probabilities and the average number of iterations before absorption. It is clear that similar variations of ν_0 will induce the same effect for populations of multicell cellicules (taking into account the partitionability of cellicules in elementary cellicules).

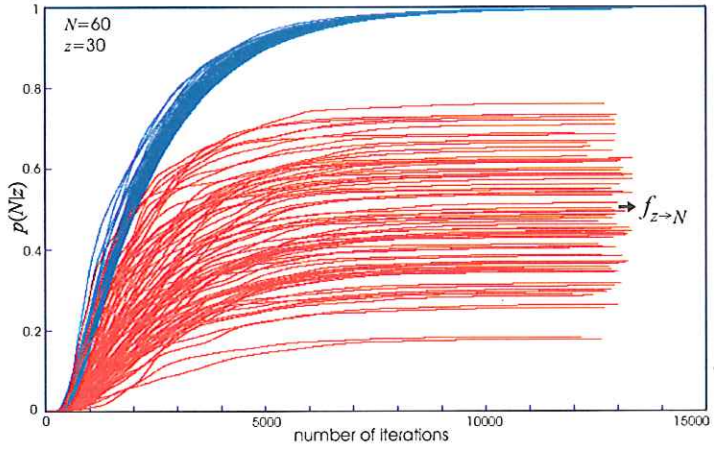


Figure 10: The Z_1-algorithm acting on a population of 60 single-cell cellicules, when ν_0 varies randomly and independently according to a uniform distribution in [0,1]. Evolution of $p(N|z)$, the probability of reaching the equilibrium state $N = 60$ starting from state $z = 30$, versus the number of iterations. A bundle of curves obtained from 80 runs is shown. The red curves show $p(N|z)$, the blue curves $p_{\text{abs}} = p(N|z) + p(0|z)$ (i.e. the probability of having reached one of the two absorbing states 0 or N). The end points of the curves occur at a number of iterations where $p_{\text{abs}} = 0.999$.

Partitioning a population Consider a population $\mathcal{P}$ of N single-cell cellicules, starting in an initial state z. Partition $\mathcal{P}$ in two subpopulations A and B, with respective number of cellicules N_A and N_B, and initial states z_A and z_B. Obviously $N = N_A + N_B$ and $z = z_A + z_B$. First let A evolve under the Z_1- algorithm, until an equilibrium population A_{eq} is reached. A_{eq} has either state $z_{A_{\text{eq}}} = 0$ or $z_{A_{\text{eq}}} = N_A$. We denote this as $\mathbf{z}_{A_{\text{eq}}}$, whereby the boldness of $\mathbf{z}$ indicates the random character of this equilibrium state ($\mathbf{z}_{A_{\text{eq}}}$

is a random variable with two possible outcomes 0 and N_A. The probability that $\mathbf{z}_{A_{\rm eq}} = 0$ is $f^A_{z_A\to 0}$, the probability of absorption of population A into state 0 when starting in state z_A; the probability that $\mathbf{z}_{A_{\rm eq}} = N_A$ equals $f^A_{z_A\to N_A}$, the probability of absorption in state N_A). Then mix equilibrium population $A_{\rm eq}$ with B, thereby forming the population $\mathcal{P}' = A_{\rm eq} + B$ of size N, and with initial state $\mathbf{z}_{A_{\rm eq}} + z_B$, and let $\mathcal{P}'$ go to equilibrium $\mathcal{P}'_{\rm eq}$ under the Z_1- algorithm. This procedure will be called a *serial (A,B)-partitioned mixing of $\mathcal{P}$*. (Remark that $A = \mathcal{P}$, and $B = \emptyset$ is a special case which corresponds to the direct application of the Z_1-algorithm to the entire population $\mathcal{P}$). $\mathcal{P}'_{\rm eq}$ has either state 0 or N, just like $\mathcal{P}$. The following theorem shows that the absorption probabilities are invariant under all serial (A,B)-partitioned mixings.

Theorem 4.1 *Let $f^{\mathcal{P}}_{z\to 0}$ be the probability of absorption of population $\mathcal{P}$ in to state 0 when staring in the initial state z, and let $f^{A_{\rm eq}+B}_{\mathbf{z}_{A_{\rm eq}}+z_B\to 0}$ be the total probability that $\mathcal{P}' = A_{\rm eq} + B$ gets absorbed in state 0 (starting in the random state $\mathbf{z}_{A_{\rm eq}} + z_B$).*

$$f^{\mathcal{P}}_{z\to 0} = f^{A_{\rm eq}+B}_{\mathbf{z}_{A_{\rm eq}}+z_B\to 0},$$

independent of the particular partitioning A, B of $\mathcal{P}$.

Proof: According to Eqs. (25)-(26) in Appendix 2.1, we have

$$f^A_{z_A\to 0} = \frac{\zeta^{z_A} - \zeta^{N_A}}{1-\zeta^{N_A}} \tag{18}$$

$$f^A_{z_A\to N_A} = \frac{1-\zeta^{z_A}}{1-\zeta^{N_A}}. \tag{19}$$

Obviously, we can write

$$f^{A_{\rm eq}+B}_{\mathbf{z}_{A_{\rm eq}}+z_B\to 0} = f^{A_{\rm eq}+B}_{0+z_B\to 0}\cdot f^A_{z_A\to 0} + f^{A_{\rm eq}+B}_{N_A+z_B\to 0}\cdot f^A_{z_A\to N_A} \tag{20}$$

$$\overset{(18,19,\text{App.2.1})}{=} \frac{\zeta^{z_B}-\zeta^N}{1-\zeta^N}\cdot\frac{\zeta^{z_A}-\zeta^{N_A}}{1-\zeta^{N_A}} + \frac{\zeta^{z_B+N_A}-\zeta^N}{1-\zeta^N}\cdot\frac{1-\zeta^{z_A}}{1-\zeta^{N_A}} \tag{21}$$

$$= \frac{\zeta^{z_0}-\zeta^N}{1-\zeta^N} \tag{22}$$

$$= f^{\mathcal{P}}_{z_0\to 0}. \tag{23}$$

■

It is also possible to consider *successive serial mixings*, as follows. Instead of letting the Z_1-algorithm act upon the mixture $\mathcal{P}' = \mathcal{A}_{\rm eq} + \mathcal{B}$, we can partition $\mathcal{P}'$ into $\mathcal{C}$ and $\mathcal{D}$, bring $\mathcal{C}$ to equilibrium $\mathcal{C}_{\rm eq}$, and finally apply the algorithm to the population $\mathcal{P}'' = \mathcal{C}_{\rm eq} + \mathcal{D}$, until a global equilibrium is reached.

Corollary 4.2 *The absorption probabilities for a population $\mathcal{P}$ of N single-cell cellicules is invariant under a successive serial mixing.*

Proof: $\mathcal{C}_{\rm eq} + \mathcal{D}$ relates to $\mathcal{P}' = \mathcal{A}_{\rm eq} + \mathcal{B}$, as $P' = \mathcal{A}_{\rm eq} + \mathcal{B}$ relates to $\mathcal{P}$. As a consequence of (22) and (23), we can write

$$f^{A_{\rm eq}+B}_{0+z_B\to 0} = \frac{\zeta^{z_B}-\zeta^N}{1-\zeta^N}, \text{ and } f^{A_{\rm eq}+B}_{N_A+z_B\to 0} = \frac{\zeta^{z_B+N_A}-\zeta^N}{1-\zeta^N}.$$

Inserting this in (20) gives exactly (21), which, by (23) equals $f^{\mathcal{P}}_{z_0\to 0}$.

■

One could even continue this successive serial mixing procedure by partitioning $\mathcal{P}''$ into $\mathcal{E}, \mathcal{F}$, creating $\mathcal{E}_{\text{eq}} + \mathcal{F}$, etcetera. As long as this ends in a final stage at which the two partitions (one being always in equilibrium) get completely mixed, the overall absorption probabilities remain invariant under whatever successive partitioning.

The following *multipartitioning* case is clearly a special instance of the successive partitioning above. It starts by partitioning the original population $\mathcal{P}$ into several disjoint subpopulations $\mathcal{P}_1, \mathcal{P}_2, \ldots, \mathcal{P}_{W-1}, \mathcal{P}_W$, all with corresponding initial state. Then apply the Z_1-algorithm to $\mathcal{P}_1$ until it gets into equilibrium $\mathcal{P}_{1,\text{eq}}$, after which $\mathcal{P}_{1,\text{eq}}$ interacts with $\mathcal{P}_2$, until it reaches the equilibrium population $(\mathcal{P}_{1,\text{eq}} \cup \mathcal{P}_2)_{\text{eq}}$. Then $(\mathcal{P}_{1,\text{eq}} \cup \mathcal{P}_2)_{\text{eq}}$ mixes with $\mathcal{P}_3$, again until an equilibrium is reached. Then this equilibrium mixes with $\mathcal{P}_4$. This procedure is continued in an obvious way until all subpopulations have participated in the serial mixing, and the total absorption probability is independent of the particular partitionings.

One can even consider the following *parallel* (A, B)*-partitioned mixing.*First split $\mathcal{P}$ into two subpopulations $\mathcal{A}$ and $\mathcal{B}$. Let the Z_1-algorithm act separately on both subpopulations, until they reach an equilibrium state A_{eq} and B_{eq}. After that, the algorithm applies to the mixture $A_{\text{eq}} + B_{\text{eq}}$

Theorem 4.3 *In a parallel (A, B)-partitioned mixing of a population $\mathcal{P}$ of single-cell cellicules, the absorption probability $f_{z\to 0}$ (and thus also $f_{z\to N}$) is independent of the particular partitioning.*

Proof:

This is a special case of the successive serial mixing corollary 4.2. Indeed, first partition $\mathcal{P}$ into A and B, and produce $\mathcal{P}' = A_{\text{eq}} + B$. Then $(C, D) = (B, A_{\text{eq}})$ can be considered as a partitioning of $\mathcal{P}'$, in which we now let $C = B$ evolve until the equilibrium $C_{\text{eq}} = B_{\text{eq}}$ is reached. This produces the final global mixture $\mathcal{P}'' = C_{\text{eq}} + D = B_{\text{eq}} + A_{\text{eq}}$ on which the Z_1-algorithm will act until global equilibrium.

■

Again, Theorem 4.3 can be easily generalized to a partitioning of the original population in multiple subpopulations that are acted upon in parallel by the Z_1-algorithm. It is even possible to let the cellicules in the original population interact via a combination of serial and parallel partitioned mixings of subpopulations, possibly also combined with successive partitionings. Theorems 4.1 and 4.3 imply that, as far as the global probabilities for absorption in the equilibrium states are concerned, it does not matter whether some of the cellicules get grouped together and interact separately for a while, as long as *all* cellicules are finally allowed to interact with each other. Also note that a successive parallel mixing using subpopulations containing two cellicules, actually models the parallel interactions between cellicules, in analogy to what would occur in a real chemical reaction. After the pairs get into equilibrium (it takes one iteration for each pair), all cellicules are mixed together and regroup again randomly in pairs, after which the cellicules in these pairs interact again. This scenario repeats until the final equilibrium state is reached.

Consider now the situation where in an equilibrium population of many "A-individuals", one mutant with conviction B appears. From Figure 7 A, it follows that, unless ν_B is sufficiently close to 1, odds are high that this individual will reconvert to A (meaning that, when ν_B is sufficiently close to 1, the probability that all convert to B can become quite substantial). Also, the probability that all convert to B grows with increasing numbers of B-mutants.

Artificial chemistries and cellular automata that model sociodynamical processes are not new. See for example, and also for additional references, [Adamatzky, 2005].

4.2 Mixing populations of multicell cellicules

Although Theorems 4.1 and 4.3, and their extensions to multi-and successive partitionings, have been derived for populations of single-cell cellicules, the absorption probability product-property conjecture from Section 3.2.3 strongly suggests that a similar property also holds for a population of multicell cellicules under the Z_1-algorithm. And, by extension, taking into account the proper cellicule-partitioning into elementary cellicules (in contrast to the population-partitioning above), we conjecture that it also holds for a population of cellicules under any S-algorithm.

Conjecture 4.4 *Let $\mathcal{P}$ be a population of cellicules, starting in an initial population state* z. *Then the global absorption probabilities $f_{\mathbf{z}\to\alpha}$, where α is one of the equilibrium population states, is invariant under all successive partitions with serial or parallel mixing.*

Let us now consider the situation where two cellicule populations evolve *separately* until equilibrium under the same S-algorithm, thereby producing S-symmetric replicas with configuration C_1 and C_2 respectively. After that, the equilibrium populations mix. Can something be said about the relationship between the new S-symmetric pattern that will be obtained in this way, and the patterns C_1 and C_2? An idea of what generally happens is given in Figure11. It shows possible equilibrium configuration states obtained from action of the D_3-algorithm on a mixture of 50 cellicules with two distinct D_3-symmetric configurations, in different ratios. It gives an idea of how some features of the "parent"-configurations C_1 and C_2 are inherited by the new configuration.

4.3 Variations on the S-algorithm

The first two variations that follow do not change the ultimate fate: uniformity in symmetry. A third variation will bring variety under equilibrium.

(i): The "no-twin" S-algorithm.

Replace the interaction scheme $C_a + C_b \to 2R(C_a, C_b)$ in step 3 of the S-algorithm by $C_a + C_b \to R_1(C_a, C_b) + R_2(C_a, C_b)$, where R_1 and R_2 originate from two independent random copying interactions on the same parent cellicule-pair, thereby retaining only one of the two resulting identical cellicules. I.e., replace the two parent cellicules by two independently created children instead of by an identical twin. This is actually equivalent to the following interaction procedure: from the parent cellicules, create two children by copying the cells where the aligned parents have the same state, and by attributing randomly and independently 0 or 1 (with respective probability ν_0,ν_1) to each cell of the children where the corresponding parent cells have a different state. Experimental evidence shows that under this variation, the algorithm will bring the population in an equilibrium state where all cellicules have the same S-symmetric configuration.

(ii): The nested S-algorithm.

After selecting randomly two parent cellicules in the population, let the S-algorithm (twin or no-twin version) iterate on these parents until a couple of identical children emerges that have S-symmetry. Then replace the parents by the children, and select a new pair of cellicules in the population as new parents and repeat the procedure (this is actually a special case of the earlier introduced successive serial mixing). One could also choose to replace the parents by two distinct children, obtained in two independent runs of the S-algorithm on the parent pair. Again, experiments indicate that the ultimate fate

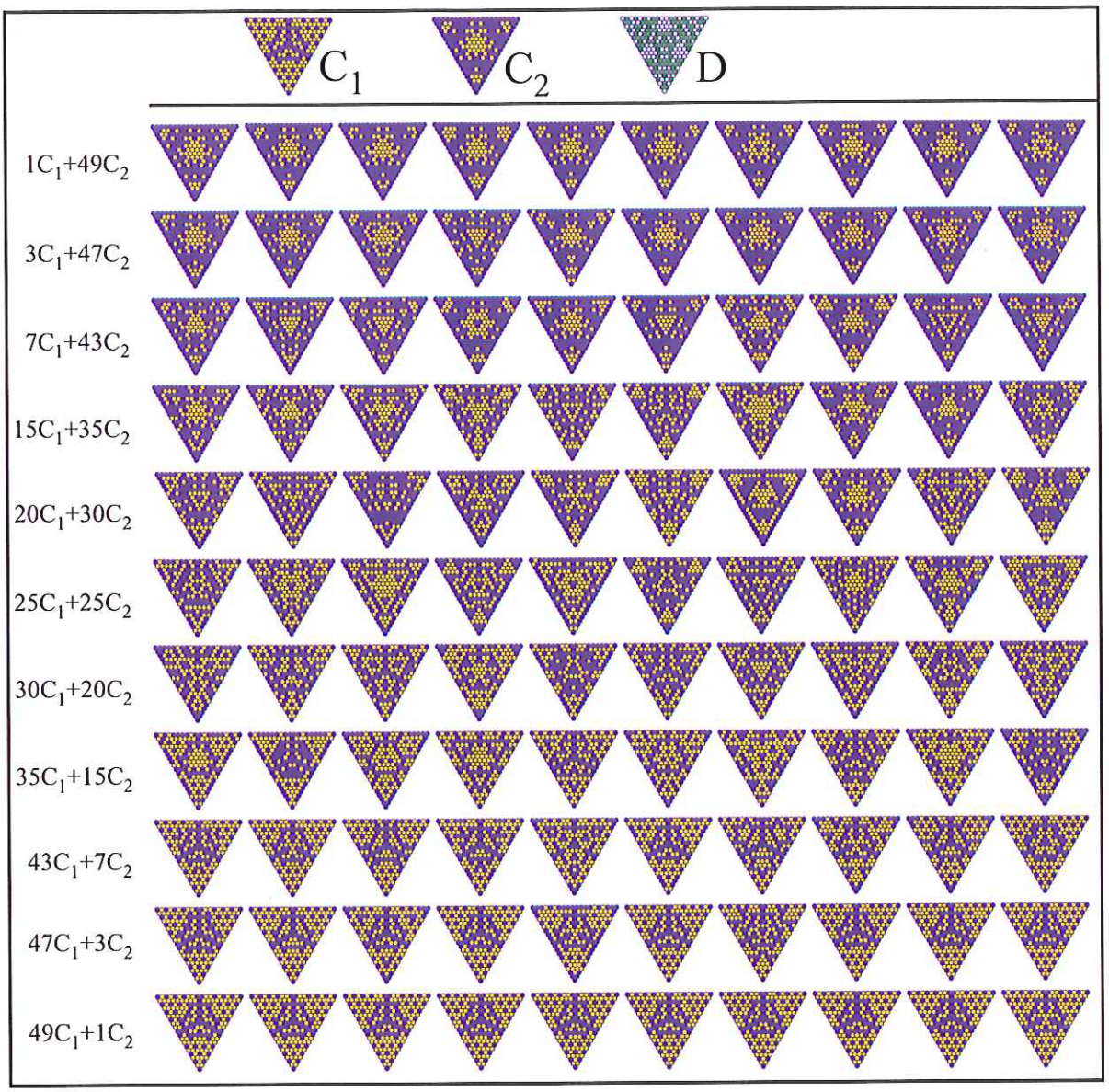


Figure 11: Configurations obtained under the D_3 algorithm from an initial population consisting of 50 cellicules of type C_1 and C_2 (having evolved themselves separately from a randomly initialized population under the D_3-algorithm).The green cells in the configuration D indicate the 114 cells where C_1 and C_2 differ. Each row presents the resulting equilibrium configuration obtained from 10 different D_3-algorithm experiments starting with an initial mixture of the form $n_1C_1 + n_2C_2$, with $n_1 + n_2 = 50$, as indicated in the first column. The equilibrium configuration clearly shows more resemblance with the configuration which has an outspoken majority in the mixture.

of these variations is also here uniformity in symmetry.

(iii): Adding interaction conditions may induce variety in the equilibrium population

It is not difficult to conceive of extra conditions on the cellicule interactions which may lead to a population with *distinct* species (configurations) which remain further invariant under the S-algorithm. An example case is provided by only allowing interactions between

cellicules which, after alignment, already have a minimal number $n_{\min}$ of cellicules in the same state. Experiments of that kind on a population of triangular cellicules subject to the D_3-algorithm, show a peculiar behavior. Let n_{brd} denote the number of cells on the triangle's border. Let $\theta = n_{\text{coinc}}/n_{\text{brd}}$ $(0 < \theta < 1)$ be the "coincidence" ratio on the n_{brd} border cells of an aligned pair of triangular cellicules (n_{coinc} denotes the number of cells where states coincide along the border). Then, experiments starting from a *randomly initialized* population of cellicules, in which an unbiased (i.e., $\nu_0 = \nu_1 = 0.5$) random copying interaction in step 3 of the S-algorithm only occurs if the actual coincidence ratio exceeds a certain treshold value θ_{t}, led to the following observation: There are two threshold values θ_{t_α}, θ_{t_β} $(\theta_{\text{t}_\alpha} < \theta_{\text{t}_\beta})$ defining three distinct zones of behavior. For $\theta < \theta_{\text{t}_\alpha}$, all cellicules in the population get into the same D_3-symmetric configuration. For $\theta > \theta_{\text{t}_\beta}$, there are no interactions (probability for the required number of coincidences being too low), and the cellicules remain in their original states (mostly only featuring the Z_1-symmetry). For $\theta_{\text{t}_\alpha} < \theta < \theta_{\text{t}_\beta}$, there is a transient zone, where the population ends up with distinct classes of identical cellicules. These classes may exhibit D_3-,Z_3-, Z_2-, Z_1-symmetry (i.e., all subsymmetries of D_3). The observations are valid for experiments in which the size of the triangular cellicules' side ranges from 5 to 30, and population sizes ranging from 25 to 10 respectively, and indicate that θ_{t_β} is close to $2/3$. Identical observations were done when broadening the coincidence condition from the border cells only, to all cells in the cellicules. Especially the transient zone is interesting, as it already brings a symmetry-breaking variety in the equilibrium state of the population. That Z_3-, Z_2- and Z_1-cellicules may appear, even under action of the D_3-algorithm, is due to the fact that the coincidence ratio treshold is not reached when such a cellicule tries to interact with any D_3-reoriented version of any other cellicule in the population (not even with a cellicule that is its own replica). Further statistical investigation is needed in order to see how θ_{t_α} and θ_{t_α} could be defined rigorously, and how they depend on the set on which the coincidence ratio is defined, on the size of this set, and on the size of the population.

These variations induce the same fatality: all cellicules which recurrently participate in the interaction will get an identical S-symmetric configuration. This ultimate monotony can only be broken by mutation and/or separate development.

4.4 Multistate cellicules

Until now, only cellicules whose cells can have two states have been considered. Several experiments have been performed in which the cells in the cellicules can have more than two states. Hereby, all steps in the S-algorithm remain the same. Only in step 3, we need to define extra copying probabilities instead of just ν_0 and ν_1. If there are M cell-states labelled $0, 1, \ldots, M-1$, and aligned cells in the selected pair of cellicules have states (α, β) $(\alpha, \beta \in \{0, 1, \ldots, M-1\}$, $\alpha \neq \beta$, the order is not important), we define $\nu_{\alpha|(\alpha,\beta)}$ and $\nu_{\beta|(\alpha,\beta)} = 1 - \nu_{\alpha|(\alpha,\beta)}$ as respective probabilities for turning both cells into state α or state β. The observation is that there is no difference in the dynamics of populations of cellicules with multistate cells: the ultimate fate remains uniformity in configuration symmetry. Figure 12 displays some configurations obtained by applying the D_4-algorithm on square cellicules with four cell-states.

The analysis for these cases is essentially similar to the cases discussed before, but becomes quickly infeasible as involving too many states, even for elementary cellicules. For example, a population of N single-cell cellicules in which cells can have a state $\in \{0, 1, 2\}$, the state space is the two-dimensional triangular domain in $\mathbb{N}^2$ defined by $P^3_{N,1} = \{(z_0, z_1) | z_0 + z_1 \leq N\}$, where $z_0, z_1, z_2 = N - z_0 - z_1$ denote the number of cellicules in state $0, 1, 2$ respectively. Again, the Z_1-algorithm induces a random-walk in this space

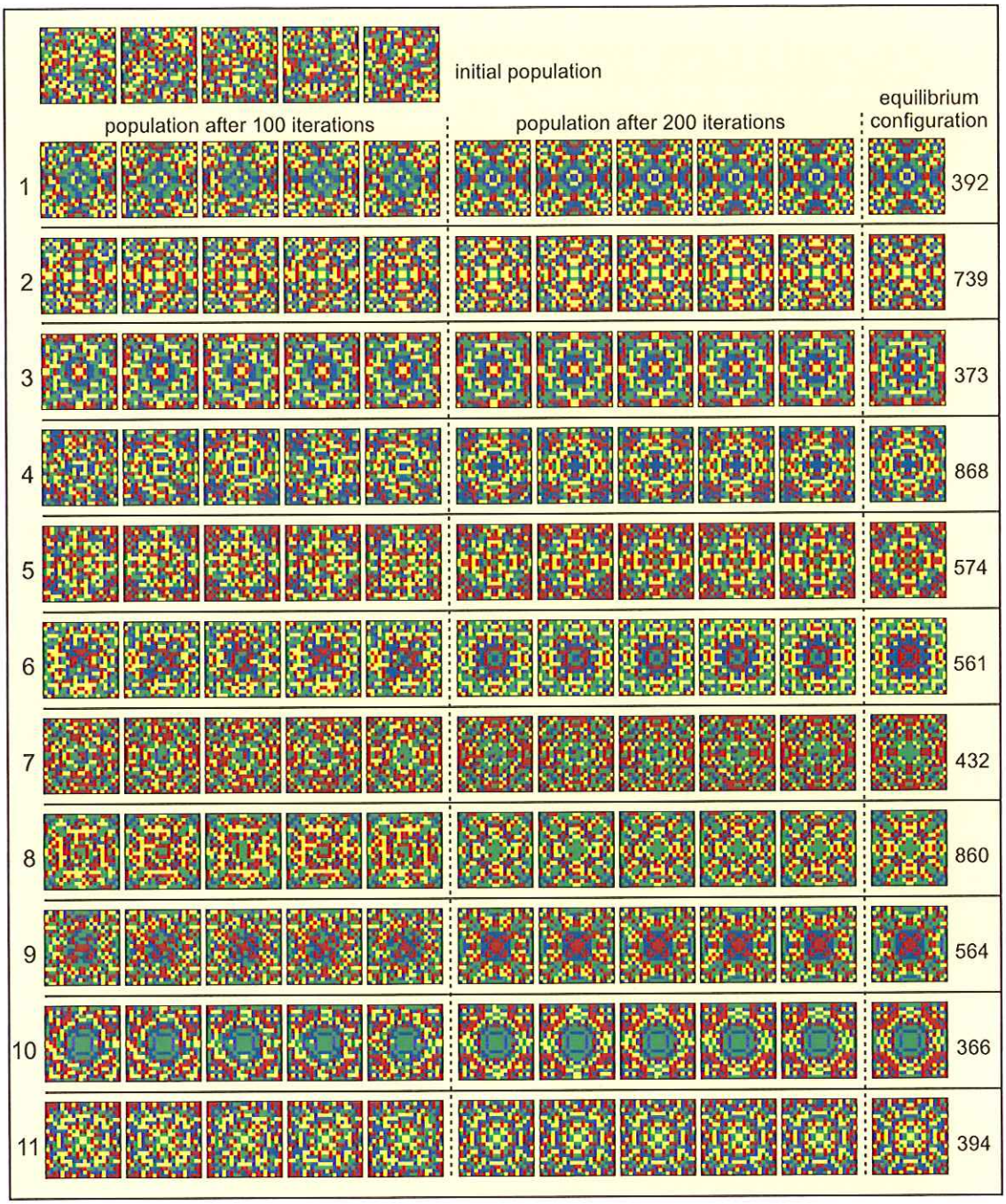


Figure 12: 1-11: different runs of the D_4-algorithm on a population of 5 square cellicules consisting of 20×20 cells. Cells are represented here as squares in one of the four states (colors) blue, green, red, yellow. These runs start with the same random initial condition displayed on top, and intermediate results for the population are shown after 100 and 200 iterations. The last column shows the configuration that all 5 cellicules reached after entering the equilibrium population state, followed by the number of iterations until equilibrium.

which is absorbed by one of the three equilibrium states $(z_0, z_1) = (N, 0), (0, N), (0, 0)$ which correspond to all cellicules having state $0, 1, 2$, respectively. Considering two-cell cellicules will already require an eight-dimensional population state space (reducible to five dimensions when considering equivalence classes under Z_2). The previously mentioned challenge to provide a generic proof that all possible cases behave as a random walk with absorbing equilibrium states, should by this be extended to include the multistate case.

5 Conclusion

We have presented a random dynamical system in the form of an artificial chemistry, with an inevitable deterministic outcome: uniformity in symmetry. The only uncertainty left about the final equilibrium state concerns the particular symmetric pattern which emerges. Despite of its random character, the S-algorithm creates order from disorder. To make it more formal: it decreases the information entropy, see e.g., [Nicolis & Nicolis, 2007]. For example, consider a population of N string cellicules of size n, subject to the Z_2-algorithm. A random initialization of the cellicules requires Nn cellicules to be randomly and independently attributed a state 0 or 1 (with equal probability 1/2). This means that there are 2^{Nn} possibilities, all with the same probability. The corresponding information entropy therefore equals

$$-\sum_{i=1}^{2^{Nn}} 2^{-Nn} \log_2 2^{-Nn} = Nn.$$

What is the information entropy for the equilibrium state, in which all elements have the same Z_2-symmetric pattern? Clearly, the remaining uncertainty at equilibrium concerns the particular Z_2-symmetric pattern of a single cellicule. When staring from a random initial condition on a population of sufficient size, no particular Z_2-symmetric pattern will be favored as outcome (i.e., the transition probabilities from a random initial population state to an absorbing state is equal for all absorbing states). As a Z_2-symmetric configuration on a string of size n requires fixing the state of $\lceil n/2 \rceil$ cells, there are $2^{\lceil n/2 \rceil}$ absorbing states, and each has a probability of $2^{-\lceil n/2 \rceil}$ of being reached. Hence the information entropy of the equilibrium state equals $\lceil n/2 \rceil$. This clearly shows that the reduction in information entropy has two causes: the appearance of replicas and the appearance of symmetry. The first one is by far the most important, certainly for larger population sizes. Calculations can be done for the Z_3 or D_3-symmetric cases, and the results are similar. The initial information entropy remains of order Nn, the final one is approximately $n|S|^{-1}$ ($|S|$ being the cardinality of the symmetry group S).

The S-algorithm shows that "chance does not exclude inevitability", in the artificial setting presented here. The quote is from Christian de Duve in his book "Life Evolving" [de Duve, 2002], where it is refers to biological evolution, thereby emphasizing that the reason for this is that chance operates under "natural" (physical/chemical) constraints. In the more limited artificial setting of the S-algorithm, these constraints lie in the underlying symmetric shape of the cellicules.

We also esteem that the importance of this cellicule-shape symmetry which constrains the random interactions for the symmetry of the resulting patterns, is of the same order as the relationship between the symmetry of the (deterministic) equations in coupled cell (oscillator) networks and the symmetry in the resulting solution (synchronization) patterns [Golubitsky & Stewart, 2002]. In the latter, symmetry-breaking in the sense that the symmetry in the solutions might be of lesser order than the symmetry in the equations seems to be common, whereas for the S-algorithm, such symmetry breaking requires additional constraints, as explained in variation *(iii)* of the algorithm (Sec. 4.3).

As mentioned in the introduction, the S-algorithm originated from an earlier study [Barbé & von Haeseler, 2003] in which triangular cellicules were completely determined by a so-called generating set of cells (forming a kind of genotype set) which, in combination with a so-called matching rule determines the overall state configuration (phenotype). In the present paper, this generating set contains all the cells in a cellicule (i.e., genotype=phenotype). We think that it is possible to formulate an S-algorithm for the more general case where this is not the case. We expect that absorption in an equilibrium state might depend in this case also on the rule which links the genotype to the phenotype.

Acknowledgements This research was supported by the FWO research community ICCoS, and the Belgian Federal Science Policy Office (IUAP P6/04 (DYSCO)).

References

Adamatzky, A. [2005] *Dynamics of Crowd-Minds. Patterns of Irrationality in Emotions, Beliefs and Actions*, World Scientific, Singapore.

Banzhaf, W. [1994] "Self-organization in a system of binary strings," in Brooks, R. & Maes, P. Eds., *Proceedings of Artificial Life IV* (MIT press, Cambridge, MA),109-118.

Barbé, A. & von Haeseler, F. [2003] "Symmetric self-organization in a cellular automaton requiring an essentially random feedback. Observations, conjectures, questions," Int. J. Bifurcation and Chaos **13**, 1029-1054.

Camazine, S., Deneubourg, J.-L., Franks, N.R., Sneyd, J., Theraulaz, G. & Bonabeau, E. [2001] *Self-Organization in Biological Systems* (Princeton University Press, Princeton).

Dawkins, R. [1986] *The Blind Watchmaker* (W. W. Norton & Company, Inc., New York).

de Duve, C. [2002] *Life Evolving*(Oxford University Press, Oxford).

de Jong, K.A. [2006] *Evolutionary Computation*, (MIT press, Cambridge, MA).

Dittrich, P., Ziegler, J. & Banzhaf, W.[2001] "Artificial chemistries - A review," Artificial Life **7**, 225-275.

Dorigo, M., & Stutzle, T. [2004] *Ant Colony Optimization*(MIT press, Cambridge, MA).

Engelbrecht, A.P. [2005] *Fundamentals of Computational Swarm Intelligence* (John Wiley & Sons, Chichester).

Golubitsky, M. & Stewart, I.[2002] *The Symmetry Perspective* (Birkhäuser Verlag, Basel)

Kaufmann, S.A. [1993] *The Origins of Order* (Oxford University Press, New-York).

Kemeny, J. & Snell, L. [1976] *Finite Markov Chains* (Springer-Verlag, New-York).

Langton, C.G. ed. [1997] *Artificial Life, An Overview*(MIT press, Cambridge, MA).

Monod, J. [1972] *Chance and Necessity: an essay on the natural philosophy of modern biology*(Collins, London).

Nicolis, G. & Nicolis, C. [2007] *Foundations of Complex Systems* (World Scientific Publishing, Singapore).

Parzen, E. [1967] *Stochastic Processes* (Holden-Day, San-Francisco) Example 6A.

Stewart, J. [2003] "Self-organization in evolution: a mathematical perspective," Phil. Trans. R. Soc. Lond. A **361**,1101-1123.

6 Appendices

Appendix 1: A physical cellicule

See Figure 13.

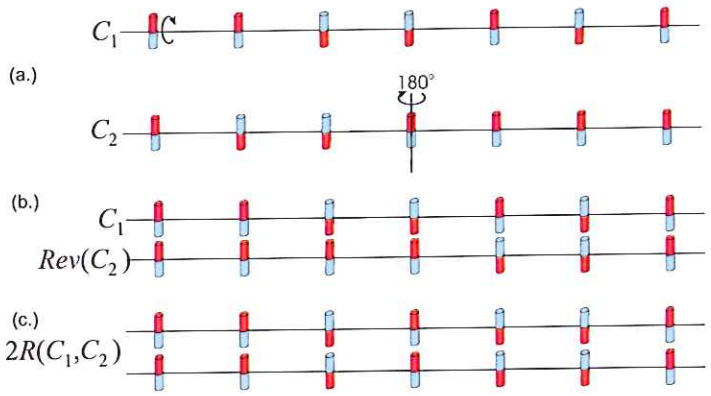


Figure 13: A concept of a physical Z_2-symmetric cellicule, in which cells are identical bar magnets, magnetically isolated (sufficiently far apart) from each other so that each individual magnet can have either up or down magnetic moment. Magnets can rotate along an horizontal axis. A cellicule may undergo a "reversal" operation by rotating it 180° along a vertical axis. Two of such devices (a) with different magnetic moment configurations can then be brought close together in perfect alignment by putting one on top of the other (b). This forces corresponding magnets in either device to stay in the same state when they already have the same state, or to randomly align to either up or down state when they originally have a different state (c). The same idea can be used for devising cellicules with Z_m-symmetric shape for use in a Z_m-Algorithm.

Appendix 2: Calculating absorption probabilities and average number of iterations before absorption

A2.1 Explicit expressions for single-cell cellicule populations

According to Eq. 6.27 in [Parzen, 1967], the probability of absorption in population state 0, starting from initial state $z \in \{0, 1, 2, \ldots, N\}$, equals

$$f_{z\to 0} = 1 - \frac{\sum_{m=0}^{z-1} \rho_m}{\sum_{m=0}^{N-1} \rho_m}, \tag{24}$$

where

$$\rho_0 = 1, \quad \rho_m = \frac{q_m \cdots q_1}{p_m \cdots p_1} \overset{(13-14)}{=} \zeta^m,$$

with

$$\zeta = \frac{\nu_1}{\nu_0}.$$

This gives, when $\zeta \neq 1$

$$f_{z\to 0} = \frac{\zeta^z - \zeta^N}{1 - \zeta^N}. \tag{25}$$

By symmetry (replace z by $N - z$, ζ by ζ^{-1}), the probability for absorption by state N is (for $\zeta \neq 1$)

$$f_{z\to N} = \frac{1 - \zeta^z}{1 - \zeta^N}. \tag{26}$$

When $\zeta = 1$, i.e. when the random copying in step 3 of the Z_1-algorithm is unbiased, these equations become

$$f_{z\to 0} = \frac{N-z}{N}, \quad f_{z\to N} = \frac{z}{N}. \tag{27}$$

Observe that the sum of both absorption probabilities equals 1. Figure 7A shows the value of $f_{z\to 0}$ versus the population state z for population size $N = 160$, with ν_0 $(= 1/(1+\zeta))$ as parameter.

The mean absorbing time $m(z, N)$ is the mean number of iterations needed in the Z_1-algorithm to bring all (single-cell) cellicules either in state 0 or state 1, starting with z cellicules in state 0 and $(N-z)$ cellicules in state 1. It can be calculated from the formulae under Example 7A in [Parzen, 1967], with the following result

(a). if $\zeta \neq 1$:

$$m(z,N) = \frac{1-\zeta^z}{1-\zeta} M_1 - \frac{N(N-1)}{2\nu_0(1-\zeta)} \sum_{j=1}^{z-1} \frac{1-\zeta^{z-j}}{j(N-j)}, \tag{28}$$

with

$$M_1 = \frac{N(N-1)}{2\nu_0(1-\zeta^N)} \sum_{j=1}^{N-1} \frac{1-\zeta^{N-j}}{j(N-j)}.$$

(b). if $\zeta = 1$ (unbiased random copying, $\nu_0 = 1/2$), these expressions become

$$m(z,N) = zM_1 - N(N-1) \sum_{j=1}^{z-1} \frac{z-j}{j(N-j)}, \tag{29}$$

with

$$M_1 = (N-1) \sum_{j=1}^{N-1} \frac{1}{j}.$$

Figure 7C shows the value of $m(z, N)$ versus the population state z for population size $N = 160$, with ν_0 as parameter.

A2.2 Using the fundamental matrix for the general case

Absorption probabilities and average absorption times can be calculated using the so-called *"fundamental matrix"* (see [Parzen, 1967] page 241, [Kemeny & Snell, 1976] §3.2, §3.3). Let P be the transition probability matrix for a Markov chain whose states are partitioned in a set T of transient states, and a set A of absorbing states. Let Q be the restriction of P to the transient states (i.e., Q is the $|T| \times |T|$ matrix obtained from P by deleting the rows and columns that correspond to an absorbing state, and keeping rows and columns corresponding to the transient states). Then the fundamental matrix is defined as

$$U = (I - Q)^{-1},$$

with I the identity matrix of the same size as Q. Let $\mathbf{m} = (m(z,N))_{z\in T}$ denote the (column) vector of the mean times to absorption from the transient states (the labels of the components of $\mathbf{m}$ range over T) and let $\mathbf{var}$ be the vector of the corresponding variances. Then it holds that

$$\mathbf{m} = U\mathbf{1}, \tag{30}$$

$\mathbf{1}$ being a column vector of proper size, with all components equal to 1. Also,

$$\mathbf{var} = U(2\mathbf{m} - \mathbf{1}) - \mathbf{m}_{\mathsf{sq}}, \tag{31}$$

where $\mathbf{m}_{\mathbf{sq}}$ denotes the vector whose components are the squares of the corresponding components of $\mathbf{m}$.

Let F be the $|T| \times |A|$ matrix of *absorption* probabilities $f_{z\to a}$ from states $z \in T$ to states $a \in A$, then

$$F = UR, \tag{32}$$

with R the part of P describing the *transition* probabilities from the transient states in T to the absorbing states in A.

Let Π be the initial probability vector for the population states, and Π_T its restriction to the set of transient states (maintaining the ordering of the components as in the matrix Q), then the global average number of iterations before absorption m_Π and corresponding variance var_Π, when starting from a randomly selected initial population state in agreement with the initial probability vector Π, are given by

$$\mathrm{m}_\Pi = \Pi_T^t \mathbf{m} \tag{33}$$

$$\mathrm{var}_\Pi = \Pi_T^t U(2\mathbf{m} - 1) - \mathrm{m}_\Pi^2 \tag{34}$$

(Π_T^t denotes the transpose of Π_T).

In the case of a population of single-cell cellicules, $A = \{0, N\}$ and $T = \{1, 2, \ldots, N-1\}$. When the states of the single-cell cellicules are initialized randomly and independently, with probability μ_0 for attributing state 0 to a cell and probability $\mu_1 = 1 - \mu_0$ for attributing state 1 (thus defining a Bernoulli trial experiment), this induces the binomial probability vector

$$\Pi_T(z) = \binom{N}{z} \mu_0^z \mu_1^{N-z} \quad (z \in T). \tag{35}$$

Figure 7E displays the global average and standard deviation of the number of iterations before absorption for this case, as a function of the population size.

Appendix 3: Efficient iterations of the S-algorithm

An efficient iteration of the S-algorithm is an iteration that results in an effective change of the population state. The *effective count* of iterations discards the iterations in the algorithm that produce the transition $z \to z$.

This effective count is linked to a new, so called *effective* Markov chain, in which the self-transitions of the transient states in the original Markov chain are deleted. According to Thm. 3.5.10 in [Kemeny & Snell, 1976], the corresponding effective transition probability matrix P_{eff} is obtained by conditioning the discrete probability function $p(x|z)$ on row z ($z = 1, \ldots, N-1$) in the probability matrix P with the event $z \nrightarrow z$. This is the event in which the population states at the start and at the end of an iteration differs. This event has probability

$$p_D = \sum_{x \neq z} p(x|z) = 1 - p(z|z). \tag{36}$$

Hence,for a population of single-cell cellicules, the discrete probability function $p(x|z)$, $x = 0, \ldots N$ as given by Eqs. (13,14,15,16), should be replaced by $p_{\mathrm{eff}}(x|z) = \frac{p(x|z)}{1-r_z}$, yielding the following transition probabilities for the transient states

$$p_{\mathrm{eff}}(z|z) \stackrel{\mathrm{def}}{=} r'_z = 0 \tag{37}$$

$$p_{\mathrm{eff}}(z+1|z) \stackrel{\mathrm{def}}{=} p'_z = \frac{p_z}{p_z + q_z} = \nu_0 \tag{38}$$

$$p_{\mathrm{eff}}(z-1|z) \stackrel{\mathrm{def}}{=} q'_z = \frac{q_z}{p_z + q_z} = \nu_1 \tag{39}$$

$$p_{\mathrm{eff}}(x|z) = 0 \text{ when } x \neq z, z+1, z-1. \tag{40}$$

For the absorbing states $z = 0$ and $z = N$, the transition probabilities $p(0|0) = 1$ and $p(N|N) = 1$ remain unchanged. All this gives the effective transition probability matrix

$$P_{\text{eff}} = \begin{bmatrix} 1 & 0 & 0 & 0 & 0 & \cdots & 0 & 0 & 0 & 0 & 0 \\ \nu_1 & 0 & \nu_0 & 0 & 0 & \cdots & 0 & 0 & 0 & 0 & 0 \\ 0 & \nu_1 & 0 & \nu_0 & 0 & \cdots & 0 & 0 & 0 & 0 & 0 \\ \vdots & & & & \vdots & \ddots & \vdots & & & & \vdots \\ 0 & 0 & 0 & 0 & 0 & \cdots & 0 & \nu_1 & 0 & \nu_0 & 0 \\ 0 & 0 & 0 & 0 & 0 & \cdots & 0 & 0 & \nu_1 & 0 & \nu_0 \\ 0 & 0 & 0 & 0 & 0 & \cdots & 0 & 0 & 0 & 0 & 1 \end{bmatrix}. \tag{41}$$

Appendix 4: Population state space of string-cellicules

The population consists of N string-cellicules of size n. A particular cellicule, say the k-th one, $k \in \{1, \ldots, N\}$ is represented by the ordered set of cells

$$C_k = [k(1), k(2), \ldots, k(n)],$$

where $k(j)$ denotes the j-th cell in the k-th cellicule. Let $s_k(j) \in \{0, 1\}$ denote the state of cell $k(j)$, then the configuration state of cellicule C_k is denoted as the binary string

$$S_k = s_k(1)s_k(2)\ldots s_k(n).$$

Let $z_{\underbrace{\alpha\beta\ldots\nu}_{n\text{digits}}}$, $\alpha, \beta, \ldots, \nu \in \{0, 1\}$ represent the number of cellicules with state $\alpha\beta\ldots\nu$, i.e.,

$$z_{\alpha\beta\ldots\nu} = |\{k|S_k = \alpha\beta\ldots\nu \in \{0,1\}^n, k \in \{1, 2, \ldots, N\}\}|.$$

Then the *population state* is given by the 2^n-vector of natural numbers

$$(z_{00\ldots00}, z_{00\ldots01}, z_{00\ldots10}, z_{00\ldots11}, \ldots, z_{11\ldots10}, z_{11\ldots11}).$$

Note that the components are indexed by the cellicule-states in lexicographic order (they form the binary equivalent of the indices $1, 2, \ldots, L$ used in the introduction). However, as the total number of cellicules is N, it follows that the sum of all components in the population state equals N, and that

$$z_{11\ldots11} = N - \sum_{\alpha\beta\ldots\nu \in \{0,1\}^n \setminus \{11\ldots11\}} z_{\alpha\beta\ldots\nu}.$$

This means that the population state can be reduced to the $(2^n - 1)$-vector

$$(z_{00\ldots00}, z_{00\ldots01}, z_{00\ldots10}, z_{00\ldots11}, \ldots, z_{11\ldots10}) \in \mathbb{N}^{2^n-1},$$

subject to the condition that the sum of all components should not exceed N. The set of all these vectors forms the (finite) population state space $P_{N,n}$.

Lemma 6.1 *The cardinality of $P_{N,n}$ equals $\binom{2^n-1+N}{2^n-1}$.*

This lemma is a direct consequence of the following lemma.

Lemma 6.2 *Consider the set Q of vectors with L components which are natural numbers, such that the sum of the components does not exceed the natural number M, i.e.,*

$$Q = \{(q_1, q_2, \ldots, q_L) \in \mathbb{N}^L | \sum_{j=1}^{L} q_j \leq M\}.$$

Then the cardinality of this set equals $|Q| = \binom{L+M}{L}$.

Proof: The proof is based on the fact that there is a bijection between the set Q and the set S of all strings of length $L+M$ featuring two symbols θ, x and containing exactly L symbols θ, i.e.,

$$S = \{s_1 s_2 \dots s_{L+M} |\, s_j \in \{\theta, \mathsf{x}\}, j = 1, \dots, L+M, \text{ number of symbols } \theta \text{ in } s_1 s_2 \dots s_{L+M} \text{ equals } L\}.$$

Indeed, let $(q_1, q_2, \dots, q_L) \in Q$, then it can be mapped into the unique S-string

$$s = \underbrace{\mathsf{x}^{q_1}\theta\mathsf{x}^{q_2}\theta\mathsf{x}^{q_3}\theta\dots\mathsf{x}^{q_L}\theta}_{\text{length of this string is } t \le L+M} \quad \mathsf{x}^{L+M-t}.$$

Note that if $q_j = 0$, then x^{q_j} is the empty string. Thus the string s has length $L+M$ and has exactly L θ's in it, and so belongs to S. For example, let $L = 5, M = 4$, then the vector $(0,1,0,2,0) \in Q$ maps into the string $\mathsf{x}^0\theta\mathsf{x}^1\theta\mathsf{x}^0\theta\mathsf{x}^2\theta\mathsf{x}^0\theta\mathsf{x} = \theta\mathsf{x}\theta\theta\mathsf{x}\mathsf{x}\theta\theta\mathsf{x}$.

On the other hand, the reverse mapping is also well defined. Given any string in S it maps into the unique vector $q = (q_1, q_2, \dots, q_L)$ where q_j equals the number of x's between the $(j-1)$-th and j-th symbol θ (q_1 is the number of x's preceding the first (leftmost) θ in the string). Clearly the sum of the components does not exceed M, as the number of x's preceding the rightmost θ does not exceed M, and thus the vector $q \in Q$.

As the cardinality of the S-set is clearly $\binom{L+M}{L}$ (L symbols out of $L+M$ must equal θ), the established bijectivity between S and Q proves that also $|Q| = \binom{L+M}{L}$.

■

Lemma 6.1 follows from Lemma 6.2 by observing that the vectors in the population state space $P_{N,n}$ have $(2^n - 1)$ components and that the sum of the components in the population state vectors does not exceed N (i.e. take $L = 2^n - 1$, $M = N$).

Appendix 5: Extended analysis of the dynamics in the population state space of two-cell cellicules under the Z_1-algorithm

According to Lemma 6.1, the population state space $P_{N,2}$ contains $\binom{3+N}{3} = O(N^3)$ states $(z_{00}, z_{01}, z_{10}) \in \{0, 1, \dots, N\}^3$ with $z_{00} + z_{01} + z_{10} \le N$ (recall that z_{ab}, $a, b \in \{0,1\}$ is the number of cellicules with state configuration ab, and that $z_{11} = N - z_{00} - z_{01} - z_{10}$).

The set of fixed points under the iterations of the Z_1-algorithm is clearly

$$\mathsf{F} = \{(0,0,0), (0,0,N), (0,N,0), (N,0,0)\}$$

(the elements of this set correspond respectively to the population states where all cellicules have configuration state 11, 01, 10, 00).

Figure 14 illustrates the structure of $P_{N,2}$: the states are the points of $\mathbb{N}^3$ which are confined to the tetrahedron OABC whose vertices are the fixed points.. Shown are the points on the faces of the tetrahedron. F_{00}, F_{01}, F_{10}, F_{11} denote (the set of points in) the faces lying respectively in the planes $z_{00} = 0$, $z_{01} = 0$, $z_{10} = 0$, $z_{11} = 0$. The set of points of $P_{N,2}$ on edge OA are the points of $P_{N,2}$ for which $z_{01} = 0$ and $z_{10} = 0$, and is denoted $E_{01,10} (= F_{01} \cap F_{10})$. In a similar way, points on the other edges OB, OC, AB, BC, CA are denoted $E_{00,10}$, $E_{00,01}$, $E_{10,11}$, $E_{00,11}$, $E_{01,11}$ respectively. For further convenience, it is useful to define also "interiors" of these sets

- $\tilde{P}_{N,2} = P_{N,2} \setminus \{F_{00} \cup F_{01} \cup F_{10} \cup F_{11}\}$: all points (states) inside the tetrahedron.
- $\tilde{F}_{00}$ = all points in the of F_{00} that do not lie on the edges. Similar for $\tilde{F}_{01}$, $\tilde{F}_{10}$, $\tilde{F}_{11}$
- $\tilde{E}_{01,10}$ = all points on edge $E_{01,10}$, except its vertices $((0,0,0), (N,0,0))$. Similar for $\tilde{E}_{00,10}$, $\tilde{E}_{00,01}$, $\tilde{E}_{10,11}$, $\tilde{E}_{00,11}$, $\tilde{E}_{01,11}$.

In order to describe the possible transitions in $P_{N,2}$, we determine the corresponding probability tree (see Fig5). Like in the single-cell case, as the only possible reorientation

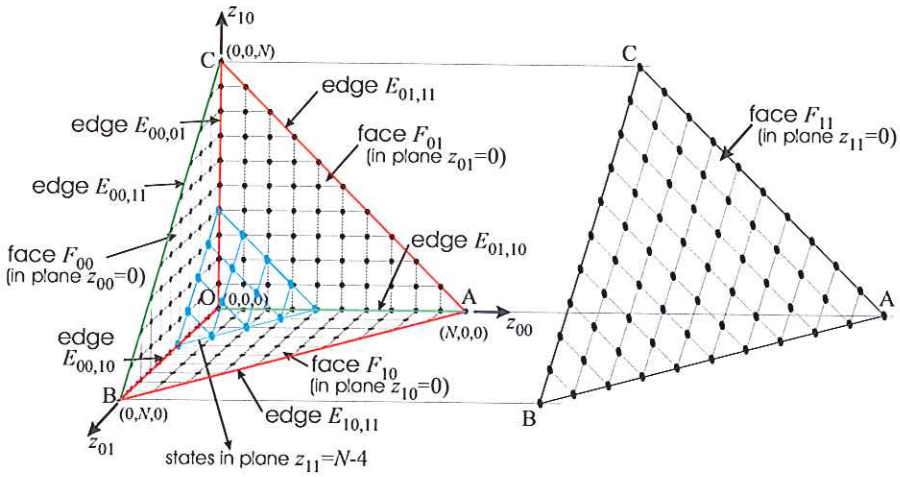


Figure 14: Structure of the population state space $P_{N,2}$ ($N = 10$).

under the Z_1-algorithm is the identity, the reorientation branches can be deleted. When ab, $a, b \in \{0, 1\}$ represents the state configuration of a two-cell cellicule, the set of possible configuration-pairs that may result from a random selection of two cellicules in step 2.1 of the algorithm, is

$$C^2_{\text{rest}} = \{(00, 00), (00, 01), (00, 10), (00, 11), (01, 01), (01, 10), (01, 11), (10, 10), (10, 11), (11, 11)\}. \tag{42}$$

The probability for a particular selection obviously depends on the population state (z_{00}, z_{01}, z_{10}), as follows

$$p_{\text{sel}}[(ab, cd)|(z_{00}, z_{01}, z_{10})] = z_{ab}z_{cd}/\binom{N}{2} = \frac{2z_{ab}z_{cd}}{N(N-1)}, \text{ in case } ab \neq cd \tag{43}$$

$$p_{\text{sel}}[(ab, ab)|(z_{00}, z_{01}, z_{10})] = \binom{z_{ab}}{2}/\binom{N}{2} = \frac{z_{ab}(z_{ab}-1)}{N(N-1)}. \tag{44}$$

(Note: whenever z_{11} appears in these expressions, it has to be replaced by $z_{11} = N - z_{00} - z_{01} - z_{10}$). In what follows, $p_{\text{sel}}[(ab, cd)|(z_{00}, z_{01}, z_{10})]$ will be shortened to $p_{\text{sel}}(ab, cd)$.

In a next step, we determine all possible outcomes from a random copying between the selected cellicule pair with configuration (ab, cd). We illustrate this for $(ab, cd) = (01, 10)$.

Random copying between the configurations 01 and 10 may produce the following pairs of cellicules

(a). $(00, 00)$: the corresponding probability for this result is $p_{\text{rc}}[(00, 00)|(01, 10)] = \nu_0^2$. This outcome induces the population state transition $(z_{00}, z_{01}, z_{10}) \to (z_{00}+2, z_{01}-1, z_{10}+1)$, and the corresponding path probability is $\nu_0^2 p_{\text{sel}}(01, 10)$.

(b). $(01, 01)$: the corresponding probability for this result is $p_{\text{rc}}[(01, 01)|(01, 10)] = \nu_0\nu_1$. This outcome induces the population state transition $(z_{00}, z_{01}, z_{10}) \to (z_{00}, z_{01}+1, z_{10}-1)$, and the corresponding path probability is $\nu_0\nu_1 p_{\text{sel}}(01, 10)$.

(c). $(10, 10)$: the corresponding probability for this result is $p_{\text{rc}}[(10, 10)|(01, 10)] = \nu_1\nu_0$. This outcome induces the population state transition $(z_{00}, z_{01}, z_{10}) \to (z_{00}, z_{01}-1, z_{10}+1)$, and the corresponding path probability is $\nu_0\nu_1 p_{\text{sel}}(01, 10)$.

(d). $(11, 11)$: the corresponding probability for this result is $p_{\text{rc}}[(11, 11)|(01, 10)] = \nu_1^2$. This outcome induces the population state transition $(z_{00}, z_{01}, z_{10}) \to (z_{00}, z_{01}-1, z_{10}-1)$, and the corresponding path probability is $\nu_1^2 p_{\text{sel}}(01, 10)$.

A similar analysis can be made for all other selections in (42). Table 1 summarizes the possible state transitions, with the corresponding transition probabilities as derived using 9 displayed in column 3 (labeled "transit.prob.")

Table 1: transitions in the population state space of N two-cell cellicules under the Z_1-algorithm.

	transition	transit.prob.	eff.prob
1	$(0,0,0) \to (0,0,0)$	1	1
2	$(0,0,N) \to (0,0,N)$	1	1
3	$(0,N,0) \to (0,N,0)$	1	1
4	$(N,0,0) \to (N,0,0)$	1	1
5	$(z_{00},z_{01},z_{10}) \to (z_{00},z_{01},z_{10})$	p_{sm} (eq.46)	0
6	$(z_{00},z_{01},z_{10}) \to (z_{00}+1,z_{01}-1,z_{10})$	$\nu_0 p_{\mathsf{sel}}(00,01)$	$\nu_0 p'_{\mathsf{sel}}(00,01)$
7	$(z_{00},z_{01},z_{10}) \to (z_{00}-1,z_{01}+1,z_{10})$	$\nu_1 p_{\mathsf{sel}}(00,01)$	$\nu_1 p'_{\mathsf{sel}}(00,01)$
8	$(z_{00},z_{01},z_{10}) \to (z_{00}+1,z_{01},z_{10}-1)$	$\nu_0 p_{\mathsf{sel}}(00,10)$	$\nu_0 p'_{\mathsf{sel}}(00,10)$
9	$(z_{00},z_{01},z_{10}) \to (z_{00}-1,z_{01},z_{10}+1)$	$\nu_1 p_{\mathsf{sel}}(00,10)$	$\nu_1 p'_{\mathsf{sel}}(00,10)$
10	$(z_{00},z_{01},z_{10}) \to (z_{00}+1,z_{01},z_{10})$	$\nu_0^2 p_{\mathsf{sel}}(00,11)$	$\nu_0^2 p'_{\mathsf{sel}}(00,11)$
11	$(z_{00},z_{01},z_{10}) \to (z_{00}-1,z_{01}+2,z_{10})$	$\nu_0\nu_1 p_{\mathsf{sel}}(00,11)$	$\nu_0\nu_1 p'_{\mathsf{sel}}(00,11)$
12	$(z_{00},z_{01},z_{10}) \to (z_{00}-1,z_{01},z_{10}+2)$	$\nu_0\nu_1 p_{\mathsf{sel}}(00,11)$	$\nu_0\nu_1 p'_{\mathsf{sel}}(00,11)$
13	$(z_{00},z_{01},z_{10}) \to (z_{00}-1,z_{01},z_{10})$	$\nu_1^2 p_{\mathsf{sel}}(00,11)$	$\nu_1^2 p'_{\mathsf{sel}}(00,11)$
14	$(z_{00},z_{01},z_{10}) \to (z_{00}+2,z_{01}-1,z_{10}-1)$	$\nu_0^2 p_{\mathsf{sel}}(01,10)$	$\nu_0^2 p'_{\mathsf{sel}}(01,10)$
15	$(z_{00},z_{01},z_{10}) \to (z_{00},z_{01}+1,z_{10}-1)$	$\nu_0\nu_1 p_{\mathsf{sel}}(01,10)$	$\nu_0\nu_1 p'_{\mathsf{sel}}(01,10)$
16	$(z_{00},z_{01},z_{10}) \to (z_{00},z_{01}-1,z_{10}+1)$	$\nu_0\nu_1 p_{\mathsf{sel}}(01,10)$	$\nu_0\nu_1 p'_{\mathsf{sel}}(01,10)$
17	$(z_{00},z_{01},z_{10}) \to (z_{00},z_{01}-1,z_{10}-1)$	$\nu_1^2 p_{\mathsf{sel}}(01,10)$	$\nu_1^2 p'_{\mathsf{sel}}(01,10)$
18	$(z_{00},z_{01},z_{10}) \to (z_{00},z_{01}+1,z_{10})$	$\nu_0 p_{\mathsf{sel}}(01,11)$	$\nu_0 p'_{\mathsf{sel}}(01,11)$
19	$(z_{00},z_{01},z_{10}) \to (z_{00},z_{01}-1,z_{10})$	$\nu_1 p_{\mathsf{sel}}(01,11)$	$\nu_1 p'_{\mathsf{sel}}(01,11)$
20	$(z_{00},z_{01},z_{10}) \to (z_{00},z_{01},z_{10}+1)$	$\nu_0 p_{\mathsf{sel}}(10,11)$	$\nu_0 p'_{\mathsf{sel}}(10,11)$
21	$(z_{00},z_{01},z_{10}) \to (z_{00},z_{01},z_{10}-1)$	$\nu_1 p_{\mathsf{sel}}(10,11)$	$\nu_1 p'_{\mathsf{sel}}(10,11)$
22	$(z_{00},z_{01},z_{10}) \to (x_{00},x_{01},x_{10}) \neq$ above	0	0

(45)

with p_{sm} the probability of selecting cellicules with the same configuration

$$p_{\mathsf{sm}} = \sum_{ab\in\{00,01,10,11\}} p_{\mathsf{sel}}(ab,ab) = \sum_{ab\in\{00,01,10,11\}} \frac{z_{ab}(z_{ab}-1)}{N(N-1)}. \tag{46}$$

$$p'_{\mathsf{sel}}(ab,cd) = \frac{p_{\mathsf{sel}}(ab,cd)}{1-p_{\mathsf{sm}}}. \tag{47}$$

Transitions (1) to (4) correspond to the absorbing states, they are just specific instances of transition (5).

The transition probabilities for the **effective** iteration count (see Appendix 3) are given in the 4th column of the table: they are obtained by conditioning the probabilities in column 3 by the event $(z_{00},z_{01},z_{10}) \nrightarrow (z_{00},z_{01},z_{10})$, which has probability $1-p_{\mathsf{sm}}$.

It is clear that, given a general state $(z_{00},z_{01},z_{10}) \in P_{N,2}$, a transition in the list is only possible if the corresponding probability is nonzero. And this depends on the specific position of (z_{00},z_{01},z_{10}). For example, a state on the interior face $\tilde{F}_{01}$ satisfies the conditions $z_{01}=0$, $z_{10}\neq 0$, $z_{00}\neq 0$, $z_{11}\neq 0$. This condition implies that the probabilities for transitions 6-7,14-17,18-19 are 0 (because $p_{\mathsf{sel}}(*,01)=0$ and $p_{\mathsf{sel}}(01,*)=0$ when $z_{01}=0$), and so these transitions do not occur. All other transitions (5,8-9,10-13,20-21) from a point in $\tilde{F}_{01}$ have probability $\neq 0$ (under the obvious assumption that $\nu_0,\nu_1\neq 0$).

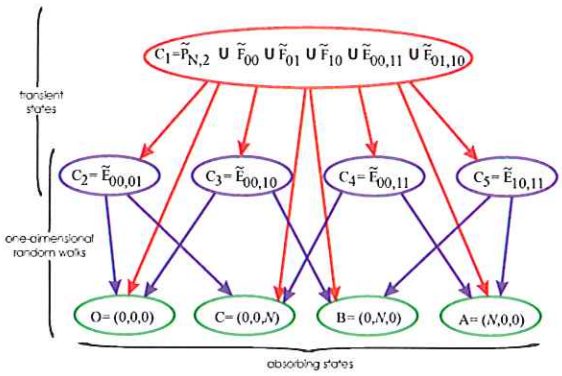


Figure 15: The hierarchy of communicating classes in the two-dimensional random walk induced by the Z_1-Algorithm in a population of N two-cell cellicules. C_1 to C_5 are distinct communicating classes. A communicating class is a maximal set of states in which there is a transition path between any two states. An arrow in the diagram indicates that there is at least one state in the class at the origin of the arrow which has a possible transition to a state in the class pointed at.

A careful analysis of the possible state transitions in $P_{N,2}$, using Table 1, shows that they define an absorbing Markov chain which has an hierarchy of communicating classes as illustrated in Figure 15 (a communicating class being a maximal set of states from which there is a transition path between any two states). The fixed points are seen to be absorbing states. All other states are transient. It is possible that, from a population state in C_1, an inner point is reached on one of the edges $E_{00,01}$, $E_{00,10}$, $E_{01,11}$, $E_{10,11}$. On such an edge, the population state performs a random walk and gets ultimately absorbed in one of its vertices (this corresponds to the case where one of the cells in all cellicules has reached the same (configuration) state, leaving a one-dimensional random-walk for the remaining cells)). It is also possible that from a certain state in C_1, there is a direct transition to an absorbing state. This happens exclusively in the following cases
-a) all but one cellicules already have the same configuration, and this one cellicule gets the same configuration after interaction with one of the other cellicules (e.g., $(0, N-1, 1) \in \tilde{E}_{00,11} \subset C_1 \overset{15}{\to} (0, N, 0)$) (15 refers to the transition number in table in Table 1).
-b) all but two cellicules already have the same configuration, and the two cellicules get this configuration after interaction with each other (e.g., $(1, N-2, 0) \in \tilde{P}_{N,2} \subset C_1 \overset{11}{\to} (0, N, 0)$).

The transition probability matrix of this Markov chain can be constructed using the transition probabilities in Table 1. A proper ordered labelling for the rows and columns in this matrix should be used, e.g. using the labels $(z_{00}, z_{01}, z_{10}) \in P_{N,n}$ in increasing lexicographic order. Then absorption probabilities and average number of iterations can be calculated from it (see Appendix 2).

Appendix 6: Extended analysis of the dynamics in the population state space of two joint but independent single-cell cellicule populations

Consider the simultaneous update of two independent populations A and B of N single-cell cellicules. This means that the Z_1-algorithm is applied synchronously to both populations (the random selection of the interactions pairs in step 2, and random copying in step 4 occur independently. The random copying parameters ν_0, ν_1 are the same for both).

The population state space of A is one-dimensional with state $z = z_0 \in \{0, 1, \ldots, N\}$

(the number of cellicules in state 0), and population B has state $z' = z'_0 \in \{0, 1, \ldots, N\}$. Thus the joint population state space is two-dimensional with state $(z, z') \in \{0, 1, \ldots, N\}^2$. This stae space is denoted $\hat{P}_{N,2}$. A simultaneous iteration of the Z_1-algorithm will produce a transition $(z, z') \to (x, x')$ for the joint population state, with a certain transition probability $p((x, x')|(z, z'))$. Because of the independency of the processes in the two populations, it holds that

$$[p(x, x')|(z, z')] = p(x|z)p(x'|z').$$

The transition probabilities are given in the third column of Table 2.

Table 2: transitions in the population state space of two joint populations of N single-cell cellicules under random copying

	transition	transit.prob.	eff.prob
1	$(0,0) \to (0,0)$	1	1
2	$(0,N) \to (0,N)$	1	1
3	$(N,0) \to (N,0)$	1	1
4	$(N,N) \to (N,N)$	1	1
5	$(z,z') \to (z,z')$	$r_z r_{z'}$	0
6	$(z,z') \to (z+1,z')$	$p_z r_{z'}$	$\frac{p_z r_{z'}}{1-r_z r_{z'}} = \nu_0 \alpha_{z,z'}$
7	$(z,z') \to (z-1,z')$	$q_z r_{z'}$	$\frac{q_z r_{z'}}{1-r_z r_{z'}} = \nu_1 \alpha_{z,z'}$
8	$(z,z') \to (z,z'+1)$	$r_z p_{z'}$	$\frac{r_z p_{z'}}{1-r_z r_{z'}} = \nu_0 \beta_{z,z'}$
9	$(z,z') \to (z,z'-1)$	$r_z q_{z'}$	$\frac{r_z q_{z'}}{1-r_z r_{z'}} = \nu_1 \beta_{z,z'}$
10	$(z,z') \to (z+1,z'+1)$	$p_z p_{z'}$	$\frac{p_z p_{z'}}{1-r_z r_{z'}} = \nu_0^2 \gamma_{z,z'}$
11	$(z,z') \to (z-1,z'-1)$	$q_z q_{z'}$	$\frac{q_z q_{z'}}{1-r_z r_{z'}} = \nu_1^2 \gamma_{z,z'}$
12	$(z,z') \to (z-1,z'+1)$	$q_z p_{z'}$	$\frac{q_z p_{z'}}{1-r_z r_{z'}} = \nu_0 \nu_1 \gamma_{z,z'}$
13	$(z,z') \to (z+1,z'-1)$	$p_z q_{z'}$	$\frac{p_z q_{z'}}{1-r_z r_{z'}} = \nu_0 \nu_1 \gamma_{z,z'}$
14	$(z,z') \to (x,x') \neq$ above	0	0

(48)

where $p_z, q_z, r_z, p_{z'}, q_{z'}, r_{z'}$ are given by Eqs.(13),(14),(15), and

$$\alpha_{z,z'} = \frac{(1-r_z)r_{z'}}{1-r_z r_{z'}}$$

$$\beta_{z,z'} = \frac{r_z(1-r_{z'})}{1-r_z r_{z'}}$$

$$\gamma_{z,z'} = \frac{(1-r_z)(1-r_{z'})}{1-r_z r_{z'}}.$$

The transition probabilities for the Markov process associated with the count of the effective iterations before absorption (fourth column in the table) are obtained by conditioning the probabilities on the effective event $(z, z') \nrightarrow (z, z')$ which has $1 - r_z r_{z'}$.

From Table 2, it is possible to construct the transition probability matrix for the corresponding random walk in the population state space $\hat{P}_{n,2}$. The set of absorbing population states is clearly $\{(0,0),(0,N),(N,0),(N,N)\}$, while all other states are transient and form an hierarchy of communicating classes, similar to the one in Figure 15 (now $C_1 = \{1, \ldots, N-1\}^2$, i.e. the points in the interior of the square displayed in Fig. 9(d,IV); C_2 to C_5 correspond respectively to the distinct edges of this square, without the vertices). Using the formulae in Appendix 2, the absorption probabilities and average number of iterations before absorption can be calculated.

Appendix 7: Extended analysis of the dynamics in the population state space of two-cell cellicules under the Z_2-algorithm

Clearly, the state space in which a population of N two-cell cellicules under the Z_2-algorithm evolves, is the same as for the case of two-cell cellicules under the Z_1-algorithm (Appendix 5):

$$P_{N,2} = \{(z_{00}, z_{01}, z_{10}) | z_{00} + z_{01} + z_{10} \leq N\}.$$

It is straightforward to determine the probability tree (cf. Fig 5), where now also the possible reorientation branches have to be taken into account, because of the reversal operation *Rev* in Z_2 (cf. Fig. 1A).

The possible configurations of a randomly selected pair of cellicules in the population, as obtained under step 2.1 of the Z_2-algorithm, and their selection probabilities, are the same as under application of the Z_1-algorithm(see Eqs. (42),(43) and (44)).

Assume that a selected pair has configuration (ab, cd). Step 2.2 in the algorithm transforms this pair into one of the possible reoriented pairs

$$(Id(ab), Id(cd)), (Id(ab), Rev(cd)), (Rev(ab), Id(cd), \ (Rev(ab), Rev(cd)),$$

each with probability 1/4 (induced by equal probabilities 1/2 for either selecting the identical and reverse reorientations *Id* or *Rev*). Then for each of these reoriented pairs, the result of the random interaction in step 3.1 can be determined, together with the probability for that particular result. From this, the corresponding transition and overall transition probability in the population state can be derived.

As an example, we analyze what happens when the selected pair has configuration $(01, 01)$, which occurs with probability $p_{\mathsf{sel}}(01, 01)$ (which depends on the population state (z_{00}, z_{01}, z_{10})). This will give the following random reorientations of the cellicule pair, each with reorientation probability $p_{\mathsf{reor}} = 1/4$

a. $(Id(01), Id(01)) = (01, 01)$: the result of a subsequent random copying can only give $(01, 01)$, (with probability $p_{\mathsf{rc}} = 1$). This induces the population state transition $(z_{00}, z_{01}, z_{10}) \rightarrow (z_{00}, z_{01}, z_{10})$, and the path probability for this transition following the specified selection, reorientation, and random copying is $\frac{1}{4} p_{\mathsf{sel}}(01, 01)$.

b. $(Id(01), Rev(01)) = (01, 10)$: the result of a random copying after this reorientation produces the following possible pairs of cellicules
(b1) $(00, 00)$, with probability $p_{\mathsf{rc}} = \nu_0^2$.
(b2) $(01, 01)$, with probability $p_{\mathsf{rc}} = \nu_0 \nu_1$
(b3) $(10, 10)$, with probability $p_{\mathsf{rc}} = \nu_0 \nu_1$
(b4) $(11, 11)$, with probability $p_{\mathsf{rc}} = \nu_1^2$.
(b1) induces the population state transition $(z_{00}, z_{01}, z_{10}) \rightarrow (z_{00} + 2, z_{01} - 2, z_{10})$, with path probability $\frac{1}{4} \nu_0^2 p_{\mathsf{sel}}(01, 01)$.
(b2) induces the population state transition $(z_{00}, z_{01}, z_{10}) \rightarrow (z_{00}, z_{01}, z_{10})$, with path probability $\frac{1}{4} \nu_0 \nu_1 p_{\mathsf{sel}}(01, 01)$.
(b3) induces the population state transition $(z_{00}, z_{01}, z_{10}) \rightarrow (z_{00}, z_{01} - 2, z_{10} + 2)$, with path probability $\frac{1}{4} \nu_0 \nu_1 p_{\mathsf{sel}}(01, 01)$.
(b3) induces the population state transition $(z_{00}, z_{01}, z_{10}) \rightarrow (z_{00}, z_{01} - 2, z_{10})$, with path probability $\frac{1}{4} \nu_1^2 p_{\mathsf{sel}}(01, 01)$.

c. $(Rev(01), Id(01)) = (10, 01)$: the random copying which follows this reorientation produces the same results as under item b.

d. $(Rev(01), Rev(01)) = (10, 10)$: the result of the subsequent random copying is $(10, 10)$ (with $p_{\mathsf{rc}} = 1$). It induces the population state transition $(z_{00}, z_{01}, z_{10}) \rightarrow (z_{00}, z_{01} - 2, z_{10} + 2)$, with path probability $\frac{1}{4} p_{\mathsf{sel}}(01, 01)$.

A similar analysis can be made for all possible pair selections. Table 3 summarizes the global result (obtained by using (9). Column 3 displays the transition probabilities for all interactions, column 4 the ones for the effective interactions only.

An analysis of the transitions which are possible from certain population states in $P_{N,2}$, based on Table 3, shows that they induce a random walk described by an absorbing Markov chain with two absorbing states, gathered in the set

$$\mathcal{A}' = \{(N,0,0),(0,0,0)\}.$$

These absorbing states correspond to a population where all cellicules have the same configuration 00 or 11, respectively. Note that these are the only configurations which are Z_2-symmetric. The population states $(0,N,0),(0,0,N)$ which were absorbing under the Z_1-algorithm (see Appendix 5), have now become transient under the introduction of the reverse reorientation in the Z_2-algorithm.

Contrary to the Z_1-case,the set $T' = P_{N,2} \setminus \mathcal{A}'$ of all other (transient) states forms now a single communicating class. This is a consequence of the following facts:

- a) all transitions from the Z_1-case (Table 1) also appear in Table 3, thus implying that the transitions between the classes as displayed in Figure 15 are possible.

- b) referring to Figure 15, there are now also transitions from the classes $C_2 = \tilde{E}_{00,01}$, $C_3 = \tilde{E}_{00,10}$, $C_4 = \tilde{E}_{01,11}$, $C_5 = \tilde{E}_{10,11}$ to class C_1, namely

$$\begin{array}{ll} \tilde{E}_{01,11} \overset{17,33}{\rightarrow} \tilde{F}_{11}, & \tilde{E}_{01,11} \overset{34}{\rightarrow} \tilde{F}_{01} \\ \tilde{E}_{10,11} \overset{14,23}{\rightarrow} \tilde{F}_{11}, & \tilde{E}_{10,11} \overset{24}{\rightarrow} \tilde{F}_{10} \\ \tilde{E}_{00,01} \overset{37,33}{\rightarrow} \tilde{F}_{00}, & \tilde{E}_{00,01} \overset{32}{\rightarrow} \tilde{F}_{01} \\ \tilde{E}_{00,10} \overset{31,23}{\rightarrow} \tilde{F}_{00}, & \tilde{E}_{00,10} \overset{22}{\rightarrow} \tilde{F}_{10}. \end{array}$$

  (the arrow-labels refer to corresponding transitions in Table 3; these are all "new" transitions induced by the reverse reorientation).

Again, Table 3 forms the basis for calculating the corresponding transition probability matrix. By using the fundamental matrix (Appendix A2.2), also absorption probabilities and the average number of iterations before absorption can be calculated. Some results are displayed in Figure 9(c).

Table 3: Transitions in the population state space of N two-cell cellicules under the Z_2-algorithm.

	transition	transit.prob.	eff.prob.
1	$(0,0,0) \to (0,0,0)$	1	1
2	$(N,0,0) \to (N,0,0)$	1	1
3	$(0,N,0) \to (0,N,0)$	$\frac{1}{4}+\frac{1}{2}\nu_0\nu_1$	0
4	$(0,N,0) \to (0,N-2,2)$	$\frac{1}{4}+\frac{1}{2}\nu_0\nu_1$	$\frac{1+2\nu_0\nu_1}{3-2\nu_0\nu_1}$
5	$(0,N,0) \to (2,N-2,0)$	$\frac{1}{2}\nu_0^2$	$\frac{2\nu_0^2}{3-2\nu_0\nu_1}$
6	$(0,N,0) \to (0,N-2,0)$	$\frac{1}{2}\nu_1^2$	$\frac{2\nu_1^2}{3-2\nu_0\nu_1}$
7	$(0,0,N) \to (0,0,N)$	$\frac{1}{4}+\frac{1}{2}\nu_0\nu_1$	0
8	$(0,0,N) \to (0,2,N-2)$	$\frac{1}{4}+\frac{1}{2}\nu_0\nu_1$	$\frac{1+2\nu_0\nu_1}{3-2\nu_0\nu_1}$
9	$(0,0,N) \to (2,0,N-2)$	$\frac{1}{2}\nu_0^2$	$\frac{2\nu_0^2}{3-2\nu_0\nu_1}$
10	$(0,0,N) \to (0,0,N-2)$	$\frac{1}{2}\nu_1^2$	$\frac{2\nu_1^2}{3-2\nu_0\nu_1}$
11	$(z_{00},z_{01},z_{10}) \to (z_{00},z_{01},z_{10})$	p_{ne} (eq.50)	0
12	$(z_{00},z_{01},z_{10}) \to (z_{00}+1,z_{01}-1,z_{10})$	$\nu_0 p_{\mathsf{sel}}(00,01)$	$\frac{\text{noneff.prob}}{1-p_{\mathsf{ne}}}$
13	$(z_{00},z_{01},z_{10}) \to (z_{00}-1,z_{01}+1,z_{10})$	$\frac{1}{2}\nu_1 p_{\mathsf{sel}}(00,01)$	,,
14	$(z_{00},z_{01},z_{10}) \to (z_{00}-1,z_{01}-1,z_{10}+2)$	$\frac{1}{2}\nu_1 p_{\mathsf{sel}}(00,01)$	,,
15	$(z_{00},z_{01},z_{10}) \to (z_{00}+1,z_{01},z_{10}-1)$	$\nu_0 p_{\mathsf{sel}}(00,10)$	,,
16	$(z_{00},z_{01},z_{10}) \to (z_{00}-1,z_{01},z_{10}+1)$	$\frac{1}{2}\nu_1 p_{\mathsf{sel}}(00,10)$	,,
17	$(z_{00},z_{01},z_{10}) \to (z_{00}-1,z_{01}+2,z_{10}-1)$	$\frac{1}{2}\nu_1 p_{\mathsf{sel}}(00,10)$	,,
18	$(z_{00},z_{01},z_{10}) \to (z_{00}+1,z_{01},z_{10})$	$\nu_0^2 p_{\mathsf{sel}}(00,11)$	,,
19	$(z_{00},z_{01},z_{10}) \to (z_{00}-1,z_{01}+2,z_{10})$	$\nu_0\nu_1 p_{\mathsf{sel}}(00,11)$	,,
20	$(z_{00},z_{01},z_{10}) \to (z_{00}-1,z_{01},z_{10}+2)$	$\nu_0\nu_1 p_{\mathsf{sel}}(00,11)$	,,
21	$(z_{00},z_{01},z_{10}) \to (z_{00}-1,z_{01},z_{10})$	$\nu_1^2 p_{\mathsf{sel}}(00,11)$	,,
22	$(z_{00},z_{01},z_{10}) \to (z_{00}+2,z_{01}-2,z_{10})$	$\frac{1}{2}\nu_0^2 p_{\mathsf{sel}}(01,01)$	,,
23	$(z_{00},z_{01},z_{10}) \to (z_{00},z_{01}-2,z_{10}+2)$	$(\frac{1}{4}+\frac{1}{2}\nu_0\nu_1) p_{\mathsf{sel}}(01,01)$	,,
24	$(z_{00},z_{01},z_{10}) \to (z_{00},z_{01}-2,z_{10})$	$\frac{1}{2}\nu_1^2 p_{\mathsf{sel}}(01,01)$	,,
25	$(z_{00},z_{01},z_{10}) \to (z_{00}+2,z_{01}-1,z_{10}-1)$	$\frac{1}{2}\nu_0^2 p_{\mathsf{sel}}(01,10)$	,,
26	$(z_{00},z_{01},z_{10}) \to (z_{00},z_{01}+1,z_{10}-1)$	$(\frac{1}{4}+\frac{1}{2}\nu_0\nu_1) p_{\mathsf{sel}}(01,10)$	,,
27	$(z_{00},z_{01},z_{10}) \to (z_{00},z_{01}-1,z_{10}+1)$	$(\frac{1}{4}+\frac{1}{2}\nu_0\nu_1) p_{\mathsf{sel}}(01,10)$	,,
28	$(z_{00},z_{01},z_{10}) \to (z_{00},z_{01}-1,z_{10}-1)$	$\frac{1}{2}\nu_1^2 p_{\mathsf{sel}}(01,10)$	,,
29	$(z_{00},z_{01},z_{10}) \to (z_{00},z_{01}+1,z_{10})$	$\frac{1}{2}\nu_0 p_{\mathsf{sel}}(01,11)$	,,
30	$(z_{00},z_{01},z_{10}) \to (z_{00},z_{01}-1,z_{10})$	$\nu_1 p_{\mathsf{sel}}(01,11)$	,,
31	$(z_{00},z_{01},z_{10}) \to (z_{00},z_{01}-1,z_{10}+2)$	$\frac{1}{2}\nu_0 p_{\mathsf{sel}}(01,11))$	,,
32	$(z_{00},z_{01},z_{10}) \to (z_{00}+2,z_{01},z_{10}-2)$	$\frac{1}{2}\nu_0^2 p_{\mathsf{sel}}(10,10)$	,,
33	$(z_{00},z_{01},z_{10}) \to (z_{00},z_{01}+2,z_{10}-2)$	$(\frac{1}{4}+\frac{1}{2}\nu_0\nu_1) p_{\mathsf{sel}}(10,10)$	,,
34	$(z_{00},z_{01},z_{10}) \to (z_{00},z_{01},z_{10}-2)$	$\frac{1}{2}\nu_1^2 p_{\mathsf{sel}}(10,10)$	,,
35	$(z_{00},z_{01},z_{10}) \to (z_{00},z_{01},z_{10}+1)$	$\frac{1}{2}\nu_0 p_{\mathsf{sel}}(10,11)$	,,
36	$(z_{00},z_{01},z_{10}) \to (z_{00},z_{01},z_{10}-1)$	$\nu_1 p_{\mathsf{sel}}(10,11)$	,,
37	$(z_{00},z_{01},z_{10}) \to (z_{00},z_{01}+2,z_{10}-1)$	$\frac{1}{2}\nu_0 p_{\mathsf{sel}}(10,11))$	,,
38	$(z_{00},z_{01},z_{10}) \to (x_{00},x_{01},x_{10}) \neq$ above	0	0

(49)

where

$$p_{\mathsf{ne}} = p_{\mathsf{sel}}(00,00) + p_{\mathsf{sel}}(11,11) + (\frac{1}{4}+\frac{1}{2}\nu_0\nu_1)[p_{\mathsf{sel}}(01,01) + p_{\mathsf{sel}}(10,10)]. \qquad (50)$$

Compacting the population state by considering equivalent state configurations .

Until now, we have made an explicit distinction between a cellicule with configuration 01 and a cellicule with configuration 10. This was necessary for studying the dynamics of the population under the Z_1-algorithm. But by introducing the possibility of an alignment with a reversal of one of the cellicules in steps 2.2,2.3 of the Z_2-algorithm, *having equal probability* as an alignment with either no reversal or two reversals, it seems plausible to no longer make this distinction. By defining the equivalence class $\overline{01} = \{01, 10\}$ of configuration states, it is possible to compact the population state vector (z_{00}, z_{01}, z_{10}) into the two-component vector $(z_{00}, z_{\overline{01}} = z_{01} + z_{10})$ and to consider the evolution in a *compacted population state space* (in [Kemeny & Snell, 1976], the aggregation of states is called *lumping*).

Indeed, a given transition $(z_{00}, z_{\overline{01}}) \rightarrow (z'_{00}, z'_{\overline{01}})$ in the compacted population state space can be found by combining the transitions $(z_{00}, z_{01}, z_{10}) \rightarrow (z'_{00}, z'_{01}, z'_{10})$ in Table 3 for which $z'_{01} + z'_{10} = z'_{\overline{01}}$. For example, the "no-change" transition $(z_{00}, z_{\overline{01}}) \rightarrow (z_{00}, z_{\overline{01}})$ is obtained by combining the disjoint transitions on rows 11,23,26,27,33 in Table 3. As a consequence, the probability for $(z_{00}, z_{\overline{01}}) \rightarrow (z_{00}, z_{\overline{01}})$ is the sum of the corresponding transition probabilities in column 3 on these rows of Table 3, and equals

$$p'_{\mathsf{ne}} = p_{\mathsf{ne}} + (\frac{1}{4} + \frac{1}{2}\nu_0\nu_1)[2p_{\mathsf{sel}}(01, 10) + p_{\mathsf{sel}}(01, 01) + p_{\mathsf{sel}}(10, 10)] \tag{51}$$

$$\overset{(50)}{=} p_{\mathsf{sel}}(00, 00) + p_{\mathsf{sel}}(11, 11) + (\frac{1}{2} + \nu_0\nu_1)p_{\mathsf{sel}}(\overline{01}, \overline{01}), \tag{52}$$

where

$$p_{\mathsf{sel}}(\overline{01}, \overline{01}) = p_{\mathsf{sel}}(01, 10) + p_{\mathsf{sel}}(01, 01) + p_{\mathsf{sel}}(10, 10) \tag{53}$$

As a matter of fact, $p_{\mathsf{sel}}(\overline{01}, \overline{01})$ equals the probability of selecting two cellicules from the class $\overline{01}$, and using (43) and (44), it can be shown that

$$p_{\mathsf{sel}}(\overline{01}, \overline{01}) = \frac{z_{\overline{01}}(z_{\overline{01}} - 1)}{N(N-1)} \tag{54}$$

(as it should indeed, thus making $p_{\mathsf{sel}}(\overline{01}, \overline{01})$ completely expressible in terms of the components $z_{00}, z_{\overline{01}}$ of the compacted population state only).

Table 4 gives the possible transitions (noneffective and and their probabilities in the compacted population state space. The numbers between brackets in the first column refer to the rows from Table 3 that have been combined. The effective transition probabilities in column 4 are again obtained by excluding the transition in which no change in the population state occurs.

Table 4: Transitions in the compacted population state space of N two-cell cellicules under mixed-alignment random copying

	transition	transit.prob.	eff.prob.
1	$(0,0) \to (0,0)$	1	1
2	$(N,0) \to (N,0)$	1	1
3	$(0,N) \to (0,N)$	$\frac{1}{2}+\nu_0\nu_1$	0
4	$(0,N) \to (0,N-2)$	$\frac{1}{2}\nu_1^2$	$\frac{\nu_1^2}{1-2\nu_0\nu_1}$
5	$(0,N) \to (2,N-2)$	$\frac{1}{2}\nu_0^2$	$\frac{\nu_0^2}{1-2\nu_0\nu_1}$
6(11, 23, 26, 27, 33)	$(z_{00}, z_{\overline{01}}) \to (z_{00}, z_{\overline{01}})$	p'_{ne}	0
7(12, 15)	$(z_{00}, z_{\overline{01}}) \to (z_{00}+1, z_{\overline{01}}-1)$	$\nu_0 p_{\mathsf{sel}}(00,\overline{01})$	$\frac{\text{transit.prob}}{1-p'_{\mathsf{ne}}}$
8(13, 14, 16, 17)	$(z_{00}, z_{\overline{01}}) \to (z_{00}-1, z_{\overline{01}}+1)$	$\nu_1 p_{\mathsf{sel}}(00,\overline{01})$	,,
9(18)	$(z_{00}, z_{\overline{01}}) \to (z_{00}+1, z_{\overline{01}})$	$\nu_0^2 p_{\mathsf{sel}}(00,11)$	,,
10(19, 20)	$(z_{00}, z_{\overline{01}}) \to (z_{00}-1, z_{\overline{01}}+2)$	$2\nu_0\nu_1 p_{\mathsf{sel}}(00,11)$	,,
11(21)	$(z_{00}, z_{\overline{01}}) \to (z_{00}-1, z_{\overline{01}})$	$\nu_1^2 p_{\mathsf{sel}}(00,11)$	,,
12(22, 25, 32)	$(z_{00}, z_{\overline{01}}) \to (z_{00}+2, z_{\overline{01}}-2)$	$\frac{1}{2}\nu_0^2 p_{\mathsf{sel}}(\overline{01},\overline{01})$	,,
13(24, 28, 34)	$(z_{00}, z_{\overline{01}}) \to (z_{00}, z_{\overline{01}}-2)$	$\frac{1}{2}\nu_1^2 p_{\mathsf{sel}}(\overline{01},\overline{01})$	,,
14(29, 31, 35, 37)	$(z_{00}, z_{\overline{01}}) \to (z_{00}, z_{\overline{01}}+1)$	$\nu_0 p_{\mathsf{sel}}(\overline{01},11)$	,,
15(30, 36)	$(z_{00}, z_{\overline{01}}) \to (z_{00}, z_{\overline{01}}-1)$	$\nu_1 p_{\mathsf{sel}}(\overline{01},11)$	,,
16(38)	$(z_{00}, z_{01}, z_{10}) \to (x_{00}, x_{01}, x_{10}) \neq$ above	0	0

(55)

with

$$p_{\mathsf{sel}}(\overline{01},11) = p_{\mathsf{sel}}(01,11) + p_{\mathsf{sel}}(10,11) = \frac{2z_{\overline{01}}z_{11}}{N(N-1)} \tag{56}$$

$(z_{11} = N - z_{00} - z_{01} - z_{10} = N - z_{00} - z_{\overline{01}})$

$$p_{\mathsf{sel}}(00,\overline{01}) = p_{\mathsf{sel}}(00,01) + p_{\mathsf{sel}}(00,10) = \frac{2z_{\overline{01}}z_{00}}{N(N-1)}. \tag{57}$$

Remark that the transition probabilities for the compacted population state could also have been obtained directly by analyzing the possible transitions induced by the respective selections $(00,00)$, $(00,\overline{01})$, $(00,11)$, $(\overline{01},\overline{01})$, $(\overline{01},11)$, $(11,11)$. Such a direct way will make it still feasible to deal with the triangular cellicules under 120° rotations as will be studied in Appendix 8.

Appendix 8: Extended analysis of the dynamics in the population state space of three-cell cellicules under the Z_3-algorithm

Here we consider a population of N triangular cellicules with three cells (i.e., three-cell elementary Z_3-cellicules, see Figure 8 (A)).

Let (a,b,c), $a,b,c \in \{0,1\}$ denote the configurationof a cellicule, where a,b,c refer respectively to the state of the upper left, upper right, and bottom cell. So there are 8 possible configurations: 000, 001, 010, 011, 100, 101, 110, 111. As the possible rotations of 0°, 120° and 240° in step 2.2 of the Z_3-algorithm occur with the same probability 1/3, these configurations can be compacted into 4 equivalence classes modulo 120°-rotations (or modulo Z_3):

$$000 = \{000\},\ \overline{001} = \{001,010,100\},\ \overline{011} = \{011,101,110\},\ \text{and } 111 = \{111\}.$$

As a consequence, the population state space consists of the triples $(z_{000}, z_{\overline{001}}, z_{\overline{011}})$, with $0 \leq z_{000} + z_{\overline{001}} + z_{\overline{011}} \leq N$. The number z_{111} of cellicules with configuration 111 is a

dependent state variable, as $z_{111} = N - (z_{000} + z_{\overline{001}} + z_{\overline{011}})$. This population state space will be denoted $T_{N,3}$. It is isomorphic with the state space $P_{N,2}$ for the two-cell string-cellicule populations described in Appendices 5 and 7 (consider the mapping $000 \leftrightarrow 00$, $\overline{001} \leftrightarrow 01$, $\overline{010} \leftrightarrow 10$, $111 \leftrightarrow 11$). However, the possible state transitions and their probabilities are different.

It is still feasible to determine the probability tree for this case (cf.Fig. 5), as there are only 10 possible pair configurations to be considered in the cellicule selection step 2.1:

$$(000,000),\ (000,\overline{001}),\ (000,\overline{011}),\ (000,111),\ (\overline{001},\overline{001}),\ (\overline{001},\overline{011}),\ (\overline{001},111),\ (\overline{011},\overline{011}),\ (\overline{011},111),\ (111,111). \tag{58}$$

We determine, by way of example, the transitions in the probability tree when two cellicules step 2.1 selects two cellicules which are both in class $\overline{001}$. As usual, the probability for this particular slection is denoted $p_{\mathsf{sel}}(\overline{001},\overline{001})$ (and depends on the population state $(z_{000}, z_{\overline{001}}, z_{\overline{011}})$) .

First observe that such a selection is realized by any selection of cellicules in the corresponding equivalence classes, i.e. there are 9 possibilities. We consider the possibility $(001,001)$. The other possibilities give the same random copying results modulo 120°-rotations. Given the selected pair $(001,001)$, there is an equal probability $p_{\mathsf{reor}} = 1/3$ that the random copying will occur with a **relative rotation** between the selected cellicules over 0°(case 1), 120° (case 2), 240°(case 3).

case 1 : relative reorientation (0°). This corresponds to a random copying between the configurations 001 and 001, meaning that there is no change after interaction. This induces the population state transition

$$(z_{000}, z_{\overline{001}}, z_{\overline{011}}) \to (z_{000}, z_{\overline{001}}, z_{\overline{011}}) \text{ with path probability } \frac{1}{3}p_{\mathsf{sel}}(\overline{001},\overline{001}) \tag{59}$$

case 2 : relative reorientation (120° (counterclockwise)). This corresponds to a random copying between the configurations 001 and 010, yielding as possible results the following configurations

$(001,001)$ inducing

$$(z_{000}, z_{\overline{001}}, z_{\overline{011}}) \to (z_{000}, z_{\overline{001}}, z_{\overline{011}}) \quad \text{w. path prob. } \frac{1}{3}\nu_0\nu_1 p_{\mathsf{sel}}(\overline{001},\overline{001}) \tag{60}$$

$(010,010)$ inducing

$$(z_{000}, z_{\overline{001}}, z_{\overline{011}}) \to (z_{000}, z_{\overline{001}}, z_{\overline{011}}) \quad \text{w. path prob. } \frac{1}{3}\nu_0\nu_1 p_{\mathsf{sel}}(\overline{001},\overline{001}) \tag{61}$$

$(011,011)$ inducing

$$(z_{000}, z_{\overline{001}}, z_{\overline{011}}) \to (z_{000}, z_{\overline{001}} - 2, z_{\overline{011}} + 2) \quad \text{w. path prob. } \frac{1}{3}\nu_1^2 p_{\mathsf{sel}}(\overline{001},\overline{001}) \tag{62}$$

$(000,000)$ inducing

$$(z_{000}, z_{\overline{001}}, z_{\overline{011}}) \to (z_{000} + 2, z_{\overline{001}} - 2, z_{\overline{011}}) \quad \text{w. path prob. } \frac{1}{3}\nu_0^2 p_{\mathsf{sel}}(\overline{001},\overline{001}) \tag{63}$$

case 3 :relative reorientation ((240° (counterclockwise)). This corresponds to a random copying between the configurations 001 and 100, yielding as possible results the

following configurations

(001, 001) inducing

$$(z_{000}, z_{\overline{001}}, z_{\overline{011}}) \rightarrow (z_{000}, z_{\overline{001}}, z_{\overline{011}}) \quad \text{w. path prob. } \frac{1}{3}\nu_0\nu_1 p_{\text{sel}}(\overline{001}, \overline{001}) \quad (64)$$

(100, 100) inducing

$$(z_{000}, z_{\overline{001}}, z_{\overline{011}}) \rightarrow (z_{000}, z_{\overline{001}}, z_{\overline{011}}) \quad \text{w. path prob. } \frac{1}{3}\nu_0\nu_1 p_{\text{sel}}(\overline{001}, \overline{001}) \quad (65)$$

(101, 101) inducing

$$(z_{000}, z_{\overline{001}}, z_{\overline{011}}) \rightarrow (z_{000}, z_{\overline{001}} - 2, z_{\overline{011}} + 2) \quad \text{w. path prob. } \frac{1}{3}\nu_1^2 p_{\text{sel}}(\overline{001}, \overline{001}) \quad (66)$$

(000, 000) inducing

$$(z_{000}, z_{\overline{001}}, z_{\overline{011}}) \rightarrow (z_{000} + 2, z_{\overline{001}} - 2, z_{\overline{011}}) \quad \text{w. path prob. } \frac{1}{3}\nu_0^2 p_{\text{sel}}(\overline{001}, \overline{001}) \quad (67)$$

These results give the following population state transitions which occur through the selection in the algorithm's step 2.1 of two cellicules which are both in class $\overline{001}$ (case $(\overline{001}, \overline{001})$ in (58)).

- combining (59,60,61,64,65) gives the transition

$$(z_{000}, z_{\overline{001}}, z_{\overline{011}}) \rightarrow (z_{000}, z_{\overline{001}}, z_{\overline{011}}), \text{ w. overall path prob. } (\frac{1}{3} + \frac{4}{3}\nu_0\nu_1)p_{\text{sel}}(\overline{001}, \overline{001}) \quad (68)$$

- combining (63,67) gives the transition

$$(z_{000}, z_{\overline{001}}, z_{\overline{011}}) \rightarrow (z_{000} + 2, z_{\overline{001}} - 2, z_{\overline{011}}), \text{ w. overall path prob. } \frac{2}{3}\nu_0^2 p_{\text{sel}}(\overline{001}, \overline{001}) \quad (69)$$

- combining (62,66) gives the transition

$$(z_{000}, z_{\overline{001}}, z_{\overline{011}}) \rightarrow (z_{000}, z_{\overline{001}} - 2, z_{\overline{011}} + 2), \text{ with overall prob. } \frac{2}{3}\nu_1^2 p_{\text{sel}}(\overline{001}, \overline{001}) \quad (70)$$

Expressions (68-70) already implement the summation of paths in (9) which pass through the selected configuration $(\overline{001}, \overline{001})$.

Doing a similar analysis for the remaining 9 possible selections of pairs of cellicules as given in (58), and applying (9), we ultimately arrive at the population state transitions and corresponding transition probabilities as given in Table 5.

Table 5: Transitions in the compacted population state space of N three-cell cellicules under the Z_3-algorithm

	transition	noneff.prob.	eff.prob.
1	$(0,0,0) \to (0,0,0)$	1	1
2	$(N,0,0) \to (N,0,0)$	1	1
3	$(0,N,0) \to (0,N,0)$	$\frac{1}{3}+\frac{4}{3}\nu_0\nu_1$	0
4	$(0,N,0) \to (0,N-2,2)$	$\frac{2}{3}\nu_1^2$	$\frac{\nu_1^2}{1-2\nu_0\nu_1}$
5	$(0,N,0) \to (2,N-2,0)$	$\frac{2}{3}\nu_0^2$	$\frac{\nu_0^2}{1-2\nu_0\nu_1}$
6	$(0,0,N) \to (0,0,N)$	$\frac{1}{3}+\frac{4}{3}\nu_0\nu_1$	0
7	$(0,0,N) \to (0,2,N-2)$	$\frac{2}{3}\nu_0^2$	$\frac{\nu_0^2}{1-2\nu_0\nu_1}$
8	$(0,0,N) \to (0,0,N-2)$	$\frac{2}{3}\nu_1^2$	$\frac{\nu_1^2}{1-2\nu_0\nu_1}$
9	$(z_{000}, z_{\overline{001}}, z_{\overline{011}}) \to (z_{000}, z_{\overline{001}}, z_{\overline{011}})$	p_{ne} (eq.(71))	0
10	$(z_{000}, z_{\overline{001}}, z_{\overline{011}}) \to (z_{000}, z_{\overline{001}}, z_{\overline{011}}+1)$	$\nu_0 p_{\mathsf{sel}}(\overline{011}, 111)$	$\frac{\text{noneff.prob}}{1-p_{\mathsf{ne}}}$
11	$(z_{000}, z_{\overline{001}}, z_{\overline{011}}) \to (z_{000}, z_{\overline{001}}, z_{\overline{011}}-1)$	$\nu_1 p_{\mathsf{sel}}(\overline{011}, 111)$	,,
12	$(z_{000}, z_{\overline{001}}, z_{\overline{011}}) \to (z_{000}, z_{\overline{001}}+1, z_{\overline{011}})$	$\nu_0^2 p_{\mathsf{sel}}(\overline{001}, 111)$	,,
13	$(z_{000}, z_{\overline{001}}, z_{\overline{011}}) \to (z_{000}, z_{\overline{001}}-1, z_{\overline{011}})$	$\nu_1^2 p_{\mathsf{sel}}(\overline{001}, 111)$	,,
14	$(z_{000}, z_{\overline{001}}, z_{\overline{011}}) \to (z_{000}, z_{\overline{001}}-1, z_{\overline{011}}+2)$	$2\nu_0\nu_1 p_{\mathsf{sel}}(\overline{001}, 111)$	,,
15	$(z_{000}, z_{\overline{001}}, z_{\overline{011}}) \to (z_{000}+1, z_{\overline{001}}-1, z_{\overline{011}})$	$\nu_0 p_{\mathsf{sel}}(000, \overline{001})$	,,
16	$(z_{000}, z_{\overline{001}}, z_{\overline{011}}) \to (z_{000}-1, z_{\overline{001}}+1, z_{\overline{011}})$	$\nu_1 p_{\mathsf{sel}}(000, \overline{001})$	,,
17	$(z_{000}, z_{\overline{001}}, z_{\overline{011}}) \to (z_{000}+1, z_{\overline{001}}, z_{\overline{011}}-1)$	$\nu_0^2 p_{\mathsf{sel}}(000, \overline{011})$	,,
18	$(z_{000}, z_{\overline{001}}, z_{\overline{011}}) \to (z_{000}-1, z_{\overline{001}}+2, z_{\overline{011}}-1)$	$2\nu_0\nu_1 p_{\mathsf{sel}}(000, \overline{011})$	,,
19	$(z_{000}, z_{\overline{001}}, z_{\overline{011}}) \to (z_{000}-1, z_{\overline{001}}, z_{\overline{011}}+1)$	$\nu_1^2 p_{\mathsf{sel}}(000, \overline{011})$	,,
20	$(z_{000}, z_{\overline{001}}, z_{\overline{011}}) \to (z_{000}+1, z_{\overline{001}}, z_{\overline{011}})$	$\nu_0^3 p_{\mathsf{sel}}(000, 111)$	,,
21	$(z_{000}, z_{\overline{001}}, z_{\overline{011}}) \to (z_{000}-1, z_{\overline{001}}+2, z_{\overline{011}})$	$3\nu_0^2\nu_1 p_{\mathsf{sel}}(000, 111)$	,,
22	$(z_{000}, z_{\overline{001}}, z_{\overline{011}}) \to (z_{000}-1, z_{\overline{001}}, z_{\overline{011}}+2)$	$3\nu_0\nu_1^2 p_{\mathsf{sel}}(000, 111)$	,,
23	$(z_{000}, z_{\overline{001}}, z_{\overline{011}}) \to (z_{000}-1, z_{\overline{001}}, z_{\overline{011}})$	$\nu_1^3 p_{\mathsf{sel}}(000, 111)$	,,
24	$(z_{000}, z_{\overline{001}}, z_{\overline{011}}) \to (z_{000}, z_{\overline{001}}+1, z_{\overline{011}}-1)$	$(\frac{2}{3}\nu_0+\nu_0^2\nu_1) p_{\mathsf{sel}}(\overline{001}, \overline{011})$	,,
25	$(z_{000}, z_{\overline{001}}, z_{\overline{011}}) \to (z_{000}, z_{\overline{001}}-1, z_{\overline{011}}+1)$	$(\frac{2}{3}\nu_1+\nu_0\nu_1^2) p_{\mathsf{sel}}(\overline{001}, \overline{011})$	,,
26	$(z_{000}, z_{\overline{001}}, z_{\overline{011}}) \to (z_{000}+2, z_{\overline{001}}-1, z_{\overline{011}}-1)$	$\frac{1}{3}\nu_0^3 p_{\mathsf{sel}}(\overline{001}, \overline{011})$	,,
27	$(z_{000}, z_{\overline{001}}, z_{\overline{011}}) \to (z_{000}, z_{\overline{001}}-1, z_{\overline{011}}-1)$	$\frac{1}{3}\nu_1^3 p_{\mathsf{sel}}(\overline{001}, \overline{011})$	,,
28	$(z_{000}, z_{\overline{001}}, z_{\overline{011}}) \to (z_{000}+2, z_{\overline{001}}-2, z_{\overline{011}})$	$\frac{2}{3}\nu_0^2 p_{\mathsf{sel}}(\overline{001}, \overline{001})$	,,
29	$(z_{000}, z_{\overline{001}}, z_{\overline{011}}) \to (z_{000}, z_{\overline{001}}-2, z_{\overline{011}}+2)$	$\frac{2}{3}\nu_1^2 p_{\mathsf{sel}}(\overline{001}, \overline{001})$	,,
30	$(z_{000}, z_{\overline{001}}, z_{\overline{011}}) \to (z_{000}, z_{\overline{001}}+2, z_{\overline{011}}-2)$	$\frac{2}{3}\nu_0^2 p_{\mathsf{sel}}(\overline{011}, \overline{011})$	,,
31	$(z_{000}, z_{\overline{001}}, z_{\overline{011}}) \to (z_{000}, z_{\overline{001}}, z_{\overline{011}}-2)$	$\frac{2}{3}\nu_1^2 p_{\mathsf{sel}}(\overline{011}, \overline{011})$	,,
32	$(z_{000}, z_{\overline{001}}, z_{\overline{011}}) \to (x_{000}, x_{\overline{001}}, x_{\overline{011}}) \neq$ above	0	0

where

$$p_{\mathsf{ne}} = p_{\mathsf{sel}}(000,000) + p_{\mathsf{sel}}(111,111) + (\frac{1}{3}+\frac{4}{3}\nu_0\nu_1)[p_{\mathsf{sel}}(\overline{001},\overline{001}) + p_{\mathsf{sel}}(\overline{011},\overline{011})] \quad (71)$$

and, with $\alpha, \beta \in \{000, \overline{001}, \overline{011}, 111\}$:

$$p_{\mathsf{sel}}(\alpha,\beta) = \frac{2z_\alpha z_\beta}{N(N-1)} \text{ if } \alpha \neq \beta, \quad (72)$$

and

$$p_{\mathsf{sel}}(\alpha,\alpha) = \frac{z_\alpha(z_\alpha-1)}{N(N-1)}. \quad (73)$$

The probabilities which take only the effective interactions among the transient states into account (column 4) are given by conditioning the probabilities in column 3 on the event $(z_{000}, z_{\overline{001}}, z_{\overline{011}}) \nrightarrow (z_{000}, z_{\overline{001}}, z_{\overline{011}})$, which has probability $1 - p_{\text{ne}}$. The set of absorbing states is $\mathcal{A}'' = \{(0,0,0),(N,0,0)\}$, and its elements correspond to populations of triple-cell cellicules which all have configuration 111, respectively 000. These configurations are the only ones that have Z_3 symmetry.

From this transition table, it can again be shown that the set of transient states states $T'' = T_{N,3} \setminus \mathcal{A}''$ forms a single communicating class. This is a consequence of the following facts:

- a) under the mapping $000 \leftrightarrow 00$, $\overline{001} \leftrightarrow 01$, $\overline{010} \leftrightarrow 10$, $111 \leftrightarrow 11$, the state space $T_{N,3}$ is isomorphic to $P_{N,2}$. Under this isomorphism, all generic transitions 5-21 in Table 1 also occur in Table 5 (as transitions 9-13,15-17,19-27) Hence, the classes and transitions as given in Figure 15, also exist for the present case.
- b) referring to 15, Table 5 introduces new transitions from C_2, C_3, C_4, C_5 to class C_1, as follows

$$\begin{aligned}
&\tilde{E}_{01,11} \overset{30,18}{\rightarrow} \tilde{F}_{11}, \quad \tilde{E}_{01,11} \overset{31}{\rightarrow} \tilde{F}_{01} \\
&\tilde{E}_{10,11} \overset{29}{\rightarrow} \tilde{F}_{11} \\
&\tilde{E}_{00,01} \overset{30}{\rightarrow} \tilde{F}_{00} \\
&\tilde{E}_{00,10} \overset{14,29}{\rightarrow} \tilde{F}_{00}, \quad \tilde{E}_{00,10} \overset{28}{\rightarrow} \tilde{F}_{10}.
\end{aligned}$$

(the arrow-labels refer to the corresponding transitions in Table 5).

From Table 5, one can construct the transition probability matrix of the underlying random walk, and calculate absorption probabilities and average number of iterations before absorption.

Appendix 9: Autonomous random copying between interacting cellicules in a population of single-cell cellicules

Replace the standard interaction between two cells in step 3.1 in the Z_1-algorithm by the following:

- if both cells are in the same state: nothing changes
- if both cells are in a different state: the cell in state 0 changes to state 1 with probability $\nu_{0\to 1}$ (and keeps state 0 with probability $\nu_{0\to 0} = 1 - \nu_{0\to 1}$), while the cell in state 1 changes to state 0 with probability $\nu_{1\to 0}$ (and keeps state 1 with probability $\nu_{1\to 1} = 1 - \nu_{1\to 0}$).

The probability tree of Figure 6 changes into the one of Figure 16. With $\theta_0 = \nu_{0\to 0}\nu_{1\to 0}$ and $\theta_1 = \nu_{0\to 1}\nu_{1\to 1}$,this gives the following population state transition probabilities:

$$p(z+1|z) \overset{\text{def}}{=} p''_z = \frac{2\theta_0 z(N-z)}{N(N-1)} \tag{74}$$

$$p(z-1|z) \overset{\text{def}}{=} q''_z = \frac{2\theta_1 z(N-z)}{N(N-1)} \tag{75}$$

$$p(z|z) \overset{\text{def}}{=} r''_z = 1 - p''_z - q''_z \tag{76}$$

$$p(x|z) = 0 \text{ when } x \neq z, z+1, z-1. \tag{77}$$

These values have to replace the corresponding transition probabilities p_z, q_z, r_z in the probability transition matrix (17). As far as absorption probabilities are concerned, it follows from (24) that the formulas (25) (26) remain valid, but now ζ has the value $\zeta = \frac{\theta_1}{\theta_0}$. Also the formulae for the mean number of iterations before absorption(28)(29),remain valid under replacement of ν_0 by θ_0. Taking only the effective interactions into account which

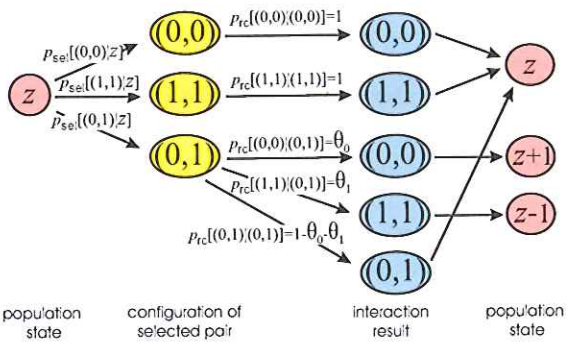


Figure 16: The complete probability tree underlying the evolution of a population of single-cell cellicules with autonomous random copying.

induce a definite change in the population state, these are based on the effective transition probabilities

$$p_{\text{eff}}(z+1|z) \overset{\text{def}}{=} p_z''' = \frac{p_z''}{1-r_z''} = \frac{\theta_0}{\theta_0+\theta_1} \tag{78}$$

$$p_{\text{eff}}(z-1|z) \overset{\text{def}}{=} q_z''' = \frac{q_z''}{1-r_z''} = \frac{\theta_1}{\theta_0+\theta_1} \tag{79}$$

$$p_{\text{eff}}(z|z) \overset{\text{def}}{=} r_z''' = 0. \tag{80}$$

This implies that ν_0 and ν_1 in the transition probability matrix (41) and in the absorption time formula (28) should be replaced by $\frac{\theta_0}{\theta_0+\theta_1}$ and $\frac{\theta_1}{\theta_0+\theta_1}$, respectively.

Caption of Figure 9:
Column IV shows the population state spaces for populations of elementary cellicules (displayed in column II), and acted upon by the S-algorithm (S mentioned in column III). The population size $N = 10$. States displayed in red are the absorbing (equilibrium) states. The population state spaces are identical for **b**,**c**,**f**, but the random walk induced by the corresponding S-algorithm differs. In some of the higher dimensional spaces, there are absorbing one-dimensional random walks: for **b** on OC,OB,CA,AB; for **d** on OC, OB, CA, AB. Column V displays the absorption probability $f_{z\to \mathsf{A}}$ for going from state z in the population state space to absorbing state A under the unbiased random copying condition $\nu_0 = \nu_1 = 0.5$. The value of $f_{z\to \mathsf{A}}$ is colorcoded, and for **d**,**e**, it is also displayed as the vertical coordinate value. The closer z is to A, the higher the probability of being absorbed by A. The absorption probabilities for other equilibrium states give an identical picture under proper reorientation of the tetrahedron OABC. Column VI shows m_z, the average number of iterations before absorption in one of the equilibrium states, when starting from an initial state z (also under the condition $\nu_0 = \nu_1 = 0.5$). Starting closer to a particular equilibrium state will on average require less iteration steps to reach an equilibrium state (with high probability this will be that particular equilibrium state). The images remain qualitatively similar for other population sizes N. For the absorption probabilities in column V, the pictures also remain qualitatively invariant under renormalization $z \to z/N$, just like for the case under **a**. This is made clear in **d**,**e**, where values are shown for $N = 10$ (the "fat" dots) and $N = 30$ (the "thin" dots). The mean number of iterations m_z in column VI tends to grow quadratically with N for constant z/N (similar to the case under **a**).